View-based Explanations for Graph Neural Networks

TINGYANG CHEN*, Zhejiang University, China
DAZHUO QIU*, Aalborg University, Denmark
YINGHUI WU, Case Western Reserve University, USA
ARIJIT KHAN, Aalborg University, Denmark
XIANGYU KE, Zhejiang University, China
YUNJUN GAO, Zhejiang University, China

Generating explanations for graph neural networks (GNNs) has been studied to understand their behaviors in analytical tasks such as graph classification. Existing approaches aim to understand the overall results of GNNs rather than providing explanations for specific class labels of interest, and may return explanation structures that are hard to access, nor directly queryable. We propose GVEX, a novel paradigm that generates **G**raph **V**iews for GNN **EX**planation. **(1)** We design a two-tier explanation structure called *explanation views*. An explanation view consists of a set of graph patterns and a set of induced explanation subgraphs. Given a database $\mathcal{G}$ of multiple graphs and a specific class label l assigned by a GNN-based classifier $\mathcal{M}$, it concisely describes the fraction of $\mathcal{G}$ that best explains why l is assigned by $\mathcal{M}$. **(2)** We propose quality measures and formulate an optimization problem to compute optimal explanation views for GNN explanation. We show that the problem is Σ_P^2-hard. **(3)** We present two algorithms. The first one follows an *explain-and-summarize* strategy that first generates high-quality explanation subgraphs which best explain GNNs in terms of feature influence maximization, and then performs a summarization step to generate patterns. We show that this strategy provides an approximation ratio of $\frac{1}{2}$. Our second algorithm performs a single-pass to an input node stream in batches to incrementally maintain explanation views, having an anytime quality guarantee of $\frac{1}{4}$-approximation. Using real-world benchmark data, we experimentally demonstrate the effectiveness, efficiency, and scalability of GVEX. Through case studies, we showcase the practical applications of GVEX.

CCS Concepts: • **Computing methodologies** → **Neural networks**; • **Information systems** → **Graph-based database models**.

Additional Key Words and Phrases: deep learning, graph neural networks, explainable AI, graph views, data mining, approximation algorithm

---

*Both authors contributed equally to this research.

Authors' addresses: Tingyang Chen, chenty@zju.edu.cn, Zhejiang University, Ningbo, China; Dazhuo Qiu, dazhuoq@cs.aau. dk, Aalborg University, Aalborg, Denmark; Yinghui Wu, yxw1650@case.edu, Case Western Reserve University, Cleveland, Ohio, USA; Arijit Khan, arijitk@cs.aau.dk, Aalborg University, Aalborg, Denmark; Xiangyu Ke, xiangyu.ke@zju.edu.cn, Zhejiang University, Hangzhou & Ningbo, China; Yunjun Gao, gaoyj@zju.edu.cn, Zhejiang University, Hangzhou, China.
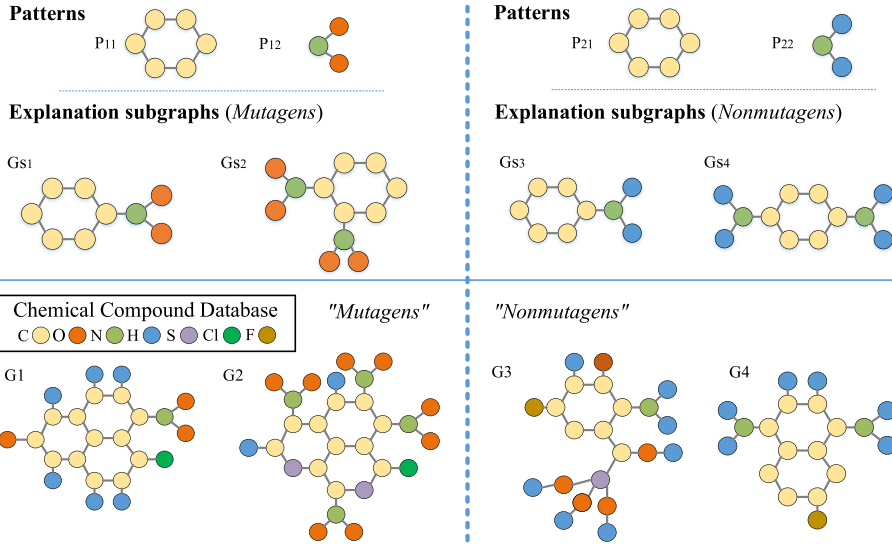

Fig. 1. GNN-based drug classification, with patterns and induced subgraphs that help understand the results.

1 INTRODUCTION

Graph classification is essential for a number of real-world tasks such as drug discovery, text classification, and recommender system [25, 52, 61]. The rising graph neural networks (GNNs) have exhibited great potential in graph classification across many real domains, e.g., social networks, chemistry, and biology [11, 51, 64, 76]. Given a database $\mathcal{G}$ as a set of graphs, and a set of class labels Ł, GNN-based graph classification aims to learn a GNN as a classifier $\mathcal{M}$, such that each graph $G \in \mathcal{G}$ is assigned a correct label $\mathcal{M}(G) \in$ Ł.

Nevertheless, it remains a desirable yet nontrivial task to explain the results of high-quality GNN-classifiers for domain experts [66]. Given $\mathcal{M}$ and $\mathcal{G}$, one wants to discover a critical fraction of $\mathcal{G}$ that is responsible for the occurrence of specific class labels of interest, assigned by GNN $\mathcal{M}$ over $\mathcal{G}$. In particular, such explanation structures should **(1)** capture both important features and topological structural information in $\mathcal{G}$; **(2)** be *queryable*, hence are easy for human experts to access and inspect with domain knowledge.

Existing GNN explanation techniques [28, 62, 65, 67, 72] primarily characterize explanations as important input features (typically in the form of numerical encodings) directly from GNN layers, and remain limited to retrieving structural information as needed [66]. These feature encodings alone cannot easily express "queryable" substructures such as subgraphs and graph patterns [67]. Indeed, graph patterns are often more intuitive to relate useful functionalities and better bridge human knowledge with GNN results. Moreover, the generated explanations typically aim to clarify all assigned labels rather than specifically addressing user-specified class labels of interest. Consider the following real-world example.

Example 1.1. In drug discovery, *mutagenicity* refers to the ability of a chemical compound to cause mutation. It is an adverse property of a molecule that hampers its potential to become a marketable drug and has been of great interest in the field. An emerging application of GNNs is to classify chemical compound as graphs in terms of mutagenicity to support effective drug discovery [30, 54].

Consider a real-world molecular dataset represented as graphs in Figure 1. A GNN classifies four graphs $\{G_1, G_2, G_3, G_4\}$ into two groups with class labels "Mutagens" and "Nonmutagens", respectively, based on whether they have mutagenicity property. A medical analyst seeks to understand

Table 1. Comparison of our GVEX technique with state-of-the-art GNN explanation methods. Here "Learning" denotes whether (node/edge mask) learning is required, "Task" means what downstream tasks each method can be applied to (GC/NC: graph/ node classification), "Target" indicates the output format of explanations (E/NF: Edge/Node Features), "Model-agnostic"(MA) means if the method treats GNNs as a black-box during the explanation stage (i.e., the internals of the GNN models are not required), "Label-specific"(LS) means if the explanations can be generated for a specific class label; "Size-bound"(SB) means if the size of explanation is bounded; "Coverage" means if the coverage property is involved (§3), "Config" means if users can configure the method to generate explanations for designated class labels (§2); "Queryable" means if the explanations are directly queryable.

Methods	LEARNING	TASK	TARGET	MA	LS	SB	COVERAGE	CONFIG	QUERYABLE
SubgraphX [67]	✗	GC/NC	Subgraph	✓	✗	✗	✗	✗	✗
GNNExplainer [62]	✓	GC/NC	E/NF	✓	✗	✗	✗	✗	✗
PGExplainer [39]	✓	GC/NC	E	✗	✗	✗	✗	✗	✗
GStarX [72]	✗	GC	Subgraph	✓	✗	✗	✗	✗	✗
GCFExplainer [28]	✗	GC	Subgraph	✓	✓	✗	✓	✗	✗
GVEX (**Ours**)	✗	GC/NC	Graph Views (Pattern+Subgraph)	✓	✓	✓	✓	✓	✓

"why" in particular the first two chemical compounds $\{G_1, G_2\}$ are recognized as mutagens, "what" are critical molecular substructures that may lead to such classification results, and further wants to search for and compare the difference between these compounds that contribute to their mutagenicity using domain knowledge. The large number of chemical graphs makes a direct inspection of GNN results challenging. For example, it is difficult to discern whether the binding of multiple carbon rings or the presence of hydrogen atoms on the carbon rings plays a decisive role in GNN-based classification to decide mutagenicity.

Based on domain knowledge, *toxicophores* are substructures of chemical compounds that indicate an increased potential for mutagenicity. For example, the aromatic nitro group is a well-known toxicophore for mutagenicity [32]. Such structures can be readily encoded as "graph views" with a two-tier structure, where toxicophores are expressed as graph patterns that summarize common substructures of a set of "explanation" subgraphs, as illustrated in Figure 1. The upper left corner of the figure shows two graph patterns $\{P_{11}, P_{12}\}$ and corresponding subgraphs that explain "why" the compounds G_1 and G_2 have mutagenicity. Indeed, we find that (1) if these subgraphs are removed from G_1 and G_2, the remaining part can no longer be recognized by the same GNN as mutagens; and (2) two of the patterns P_{11} and P_{12} are real toxicophores as verified by domain experts. Similarly, the middle right corner depicts subgraphs with common structures summarized by graph patterns P_{21} to P_{22}, which are responsible for nonmutagens. Surprisingly, P_{21} and P_{22} are also toxicophores as per domain knowledge. Therefore, such patterns can be suggested to the analysts for further inspection, or be conveniently issued as graph queries for downstream analysis, e.g., *"which toxicophores occur in mutagens?" "Which nonmutagens contain the toxicophore pattern P_{22}"?*.

In addition, the analyst wants to understand representative substructures that are discriminative enough to distinguish mutagens and nonmutagens. This can be captured by the specific toxicophore P_{12} that covers the nodes in all two chemical compounds $\{G_1, G_2\}$ with label "mutagens", but does not occur in nonmutagens $\{G_3, G_4\}$. These graph patterns, along with their matched subgraphs, provide concise and queryable structures to humans, enabling a more intuitive understanding of the GNN-based mutagenicity analysis.

The above example illustrates the need to generate queryable explanation structures which can effectively describe the fraction of graph data that are responsible for the occurrence of user-specified class labels in GNN-based classification. A desirable paradigm would **(1)** be *model-agnostic*, i.e., does not require internals of the GNNs to generate explanations; **(2)** be *specific* in distinguishing the explanations for different class labels; **(3)** be *representative* to cover important substructure of

the graphs that are assigned with the labels of interests, without over- or under-representing them (formally stated in §3); **(4)** be *configurable* to enable users with the flexibility to freely select a designated number of nodes from different classes, to obtain comprehensive and detailed explanations tailored to their classes of interest (§2); and **(5)** be *queryable* to provide direct access for human experts with (domain-aware) queries. None of the existing GNN explanation methods can address these desirable properties (Table 1).

Graph views and view selection have been studied as an effective way to access graph data [16, 41, 69]. Given a graph G, a *graph view* contains a graph pattern P and a materialized subgraph $P(G)$ that matches P via graph pattern matching. We advocate that graph views, as two-tier explanation structures, fit naturally to explain GNN-based classification. Indeed, the subgraphs possess the ability to describe the essential structure of original graphs in a manner that is both model-agnostic and configurable. The ability to configure our GVEX algorithms by ensuring a desirable amount of nodes from each class label to be covered, enables domain-expert users to extract more relevant information for their specific inquiries, as presented in our case study (§6.2). Consequently, these subgraphs inherently exhibit discriminative and informative properties for distinct classes. To enhance user inspection, we introduce patterns as a queryable structure through pattern mining, it is a summary of subgraphs and it helps domain experts inspect large-size explanations based on their higher-tier patterns, thereby facilitating easy access and analysis. We are interested in the following two questions: **(1)** *How to characterize* GNN *explanation with graph views?* and **(2)** *how can we generate graph views to extract explanations for* GNN *in a concise and configurable manner?* The answers to these questions not only provide new perspectives towards explainability, but also enable finer-grained, class label-specific analysis of GNNs.

Contributions. We summarize our main contributions as follows.

(1) We introduce *explanation views*, a novel class of explanation structure for GNN-based graph classification. An explanation view is a two-tier structure that consists of graph patterns and a set of explanation subgraphs induced from graphs via graph pattern matching, such that (a) the subgraphs are responsible for the occurrence of specific class label l of user's interest, and (b) the patterns summarize the details of explanation subgraphs as common substructures for efficient search and comparison of these subgraphs (§2).

(2) For explanation views, we introduce a set of quality measures in terms of explainability and coverage properties (§3). We formulate the problem to compute the optimal explanation views for GNN-based graph classification. The problem is in general Σ_P^2-hard, and even remains *NP*-hard for a special case when $\mathcal{G}$ has no edge.

(3) We present GVEX, an algorithmic solution for generating graph views to explain GNNs. (a) We first introduce an approximation scheme (§4) that follows an "explain-and-summarize" strategy. The method first computes a set of node-induced subgraphs with guaranteed explainability, by identifying important nodes with the maximum diversified feature influence. We then summarize these subgraphs into graph patterns that ensures to cover all such nodes, and meanwhile, introduce small edge coverage error. This guarantees an overall $\frac{1}{2}$-approximation for the view generation problem. (b) We further develop a streaming algorithm (§5) that avoids generation of all explanation subgraphs. The algorithm processes a batched stream of nodes and incrementally maintains explanation views under the coverage constraint, with an approximation ratio $\frac{1}{4}$ relative to the processed fraction of graphs.

(4) Using real-world graphs and representative GNNs, we experimentally verify that our view generation algorithms can effectively retrieve and summarize substructures to explain GNN-based classification (§6). We also showcase that our algorithms can support GNN-based drug design and social analysis well.

Related Work. We summarize the related work as follows.

Graph Neural Networks. Graph neural networks (GNNs) are deep learning models designed to tackle graph-related tasks in an end-to-end manner [53]. While GNNs have several variants (e.g., graph convolutional networks (GCNs) [35], graph attention networks (GATs) [49], graph isomorphism networks (GINs) [55], APPNP [36], and GraphSAGE [22]), they share a similar feature learning paradigm: For each node, GNNs update the features of a node by aggregating the counterparts from its neighbors to update its own features. GNNs have demonstrated their efficacy on various tasks, including node and graph classification [35, 55, 63, 71], link prediction [70].

Explanation of GNNs. Several approaches have been proposed to generate explanations for GNNs [27, 28, 39, 44, 45, 62, 65, 67, 68, 72]. Instance-level methods provide input-dependent explanations for each test graph, whereas model-level methods provide a global understanding of GNNs without considering specific input instances or class labels [66]. For example, GNNExplainer [62] learns to optimize soft masks for edges and node features to maximize the mutual information between the original and new predictions and induce important substructures from the learned masks. SubgraphX [67] explains GNN models by identifying important subgraph for an input graph. It employs Shapley values to measure a subgraph's importance by considering the interactions among different graph structures. XGNN [65] aims to explore high-level explanations of GNNs by generating graph patterns to maximize a specific prediction. GCFExplainer [28] studies the global explainability of GNNs through counterfactual reasoning. Specifically, it finds a small set of representative counterfactual graphs that explain all the input graphs rather than label-specific classes of users' interests.

However, these methods do not explicitly support configurable and queryable explanation structures, and are not optimized to generate explanations for user-specific labels. Meanwhile, they cannot be easily extended to support such constraints. First, achieving configurable property is computationally hard (Theorem 3.2), existing solutions do not address such needs, and extending them for configurability is non-trivial due to the computational hardness. Second, the "queryable" property involves extracting commonalities within explanations to facilitate direct access to critical insights, current methods generate large explanations for label explanations and stll lack the ability to include important patterns, hindering the efficient and effective computation of queryable structures. None of the prior methods supports all desirable properties at the same time, as illustrated in Table 1. Consequently, there is a need for more effective and efficient methods for explaining GNNs that can provide interpretable and accurate explanations of their predictions.

Graph Views. Graph views have been studied as a useful approach to access and query large graphs [41]. A graph view consists of a graph pattern and a set of subgraphs as its matches via graph pattern matching. Graph views are shown to be effective in view-based query processing [16], summarization [47], event analysis [73], query suggestion [40], data cleaning [37] and data pricing [10]. Several approaches have also been developed to discover graph views [37, 47].

Graph pattern mining. Graph pattern mining techniques discover frequent or other important structures within graph data [29, 42, 48, 58, 59], which can help constructing graph views and ensure generation of higher-tier patterns from lower-tier explanation subgraphs in our two-tier explanation structure. However, graph mining alone is insufficient to generate GNN explanations, e.g., consistent and counterfactual lower-tier explanations (§2.2).

To the best of our knowledge, this is the first work that exploits graph views to support queryable explanation for GNN-based classification. Our approach is a post-hoc method that treats GNNs as black-box (hence does not require details from GNNs, but only the output from its last layer), does not require node/edge mask training, and generates explanations as views that are queryable, concise, and class label-specific, all in a user-configurable manner (Table 1).

Table 2. Table of notations

Symbol	Meaning
$G = (V, E)$	Graph with nodes V and edges E
(X, A)	Feature representation of G: (X: feature matrix; A: adjacency matrix)
$\mathcal{M}; X^k$	A GNN-based classifier; the embedding of node v at layer k of $\mathcal{M}$
$\mathcal{G}; \mathcal{V}$	A set of graphs (graph database) for classification; node group of $\mathcal{G}$
$G_s^l = (V_s, E_s); \mathcal{G}_s^l$	An explanation subgraph G_s^l induced by nodes V_s w.r.t. class label l; a set of explanation subgraphs $\mathcal{G}_s^l$ w.r.t. class label l
$\mathcal{G}^l; \mathcal{V}^l$	Label group (of graphs with label l); the node set of $\mathcal{G}^l$
$P; \mathcal{P}$	A single graph pattern P; a set of graph patterns $\mathcal{P}$
$\mathcal{G}_{\mathcal{V}}^l = (\mathcal{P}^l, \mathcal{G}_s^l)$	A single explanation view with a pattern set $\mathcal{P}^l$ and an explanation subgraph set $\mathcal{G}_s^l$
$C = (\theta, r, \{[b_l, u_l]\})$	A configuration that specifies explainability (θ, r) and coverage constraints $\{[b_l, u_l]\}$ ($l \in$ Ł)
$\mathcal{G}_{\mathcal{V}}$	A set of explanation views

2 PRELIMINARIES

We start with reviewing attributed graphs, GNNs, and graph views in §2.1. We then introduce view-based explanations in §2.2. For easy reference, important notations are summarized in Table 2.

2.1 Graph Neural Networks and Graph Views

Attributed Graphs. We consider a connected graph $G = (V, E, T, L)$, where V is the set of nodes, and $E \subseteq V \times V$ a set of edges. Each node v carries a tuple $T(v)$ of attributes (or features) and their values. Each node $v \in V$ (resp. edge $e \in E$) has a *type* $L(v)$ (resp. L(e)).

Graph Neural Networks. GNNs are a family of well-established deep learning models that extend traditional neural networks to transform graphs into proper embedding representations for various downstream analysis such as graph classification. In a nutshell, GNNs employ a multi-layer message-passing scheme, through which the feature representation of a node in the next layer is aggregated from its neighborhood in the current layer. For example, the Graph Convolutional Network (GCN) [35], a representative GNN model, adopts a general form of the function as:

$$X^k = \delta(\hat{D}^{-\frac{1}{2}} \hat{A} \hat{D}^{-\frac{1}{2}} X^{k-1} \Theta^k) \tag{1}$$

Here $\hat{A} = A + I$, where I represents the identity matrix and A is the adjacency matrix of graph G. X^k indicates node feature representation in the k-th layer, (with $X^0 = X$ a matrix of input node features), where each row X_v is a vector (numerical) encoding of a node tuple $T(v)$. The encoding can be obtained by, e.g., word embedding or one-hot encoding [20]. $\hat{D}$ represents the diagonal node degree matrix of $\hat{A}$, $\delta(\cdot)$ is the non-linear activation function, and Θ^k represents the learnable weight matrix for the k-th layer.

GNN-based Classification. The task of graph classification is to correctly assign a categorical class label for a graph. Given a database (a set of graphs) $\mathcal{G} = \{G_1, G_2, \ldots, G_m\}$ and a set of class labels Ł, a GNN-*based classifier* $\mathcal{M}$ of k layers (1) takes as input $G_i = (X_i, A_i)$ ($i \in [1, m]$), learns to generate feature representations X_i^k, converts them into class labels that best fit a set of labeled graphs ("training examples"), and (2) assigns, for each unlabeled "test" graph $G_i \in \mathcal{G}$, a class label $l \in$ Ł (denoted as $\mathcal{M}(G_i) = l$).

We aim to generate queryable structures that can also clarify the class labels of user's interests assigned by a GNN-based classifier $\mathcal{M}$ over $\mathcal{G}$. To this end, we revisit graph patterns and views as "building block" structures for view-based GNN explanation.
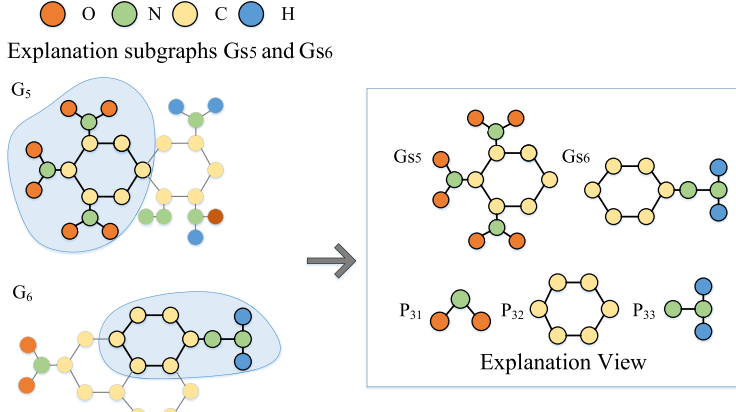
Fig. 2. An explanation view for a single class label: explanation subgraphs and patterns

Graph Patterns. A *graph pattern* is a connected graph $P(V_p, E_p, L_p)$, where V_p is a set of pattern nodes, E_p is a set of pattern edges, and L_p is a function that assigns for each node $v_p \in V_p$ (resp. edge $e_p \in E_p$) a *type* $L(v_p)$ (resp. $L(e_p)$).

Graph Pattern Matching. We use *node-induced subgraph isomorphism* [17] to characterize graph pattern matching. Given a graph G and a pattern P, there is a matching function h between P and G if for each pattern node $v_p \in V_P$, (1) $h(v_p)$ is a node in V and $L(v) = L_p(v_p)$, (2) $(h(v_p), h(v'_p))$ is an edge in G if $(v_p, v'_p) \in E_p$, and $L(h(v_p), h(v'_p)) = L_p(v_p, v'_p)$. We say that a graph pattern P *covers* a node v (resp. an edge e) if there is a matching h such that $h(v_p) = v$ (resp. $h(e_p)=e$) for some $v_p \in V_p$ (resp. $e_p \in E_p$). Given a set of graph patterns $\mathcal{P}$ and a set of graphs $\mathcal{G}$, we say that $\mathcal{P}$ *covers* the nodes (resp. edges) in $\mathcal{G}$, if for every graph $G \in \mathcal{G}$ and every node v (resp. edge e) in G, there exists a pattern $P \in \mathcal{P}$, such that P covers v (resp. e).

Graph Views. Graph views have been extensively studied to support fast graph access and query processing [41]. Given a graph database $\mathcal{G}$, we represent a graph view as a "two-tier" structure, denoted as $\mathcal{G}_V = (\mathcal{P}, \mathcal{G}_s)$, where (1) $\mathcal{P} = \{P_1, \ldots, P_n\}$ is a set of graph patterns, and (2) $\mathcal{G}_s$ is a set of connected subgraphs of the graphs from $\mathcal{G}$ which are induced by the nodes that matches the patterns in $\mathcal{P}$ via node-induced subgraph isomorphism (see "Graph Pattern Matching"). Note that by definition, $\mathcal{P}$ covers all the nodes in $\mathcal{G}_s$.

Remarks. We remark the difference between a "type" $L(\cdot)$ and a "class label" $l \in Ł$. The former refers to the real-world entity types, as seen in, e.g., ontologies, and are enforced to be consistent in graph pattern matching; and the latter refers to the task-specific class labels assigned by GNN-based classifiers. For simplicity, we shall refer to "class labels" as "labels", "GNN-based classifier" as "GNN", and "graph patterns" as "patterns".

2.2 Explanation Views

We now extend graph views as explanation structures for GNN. We start with the concept of *explanation subgraphs* to capture the fraction of a graph that is responsible for its label assigned by a GNN-based classifier $\mathcal{M}$. We then introduce view-based explanation.

Explanation Subgraphs. Given a GNN $\mathcal{M}$ and a single graph $G \in \mathcal{G}$ with label $\mathcal{M}(G) = l \in Ł$, we say that a subgraph of G is an *explanation subgraph* of G for $\mathcal{M}$ *w.r.t. a label l*, denoted as G_s^l, if

- $\mathcal{M}(G) = \mathcal{M}(G_s^l) = l$ ("*consistent*"), and
- $\mathcal{M}(G \setminus G_s^l) \neq l$ ("*counterfactual*").

Here $G \setminus G_s^l$ is the subgraph obtained by removing G_s^l from G. An explanation subgraph G_s^l of G with label l is a subgraph of G that clarifies "why" $\mathcal{M}(G) = l$ in terms of counterfactual causality [50]. That is, it is consistently assigned the same label l by $\mathcal{M}$ as G, and if "removed" from G, $\mathcal{M}$ assigns the remaining fraction of G a different label for a graph database $\mathcal{G}$ and a set of class labels Ł, one can fine-tune a set of labels of interests from Ł and generate explanation subgraphs accordingly (as will be discussed).

Explanation Views. Given a graph database $\mathcal{G}$, a GNN classifier $\mathcal{M}$, and a user-specified label of interest $l \in$ Ł, we consider a *label group* $\mathcal{G}^l \subseteq \mathcal{G}$ as the set of graphs with assigned label l. An *explanation view* of $\mathcal{G}$ for $\mathcal{M}$ w.r.t. l is a graph view $\mathcal{G}_{\mathcal{V}}^l = (\mathcal{P}^l, \mathcal{G}_s^l)$, where

- $\mathcal{G}_s^l$ is a set of explanation subgraphs of the label group $\mathcal{G}^l$, such that for each graph $G \in \mathcal{G}^l$, there is an explanation subgraph[1] G_s of G in $\mathcal{G}_s^l$ and
- $\mathcal{P}^l$ is a set of graph patterns, such that the nodes of $\mathcal{G}_s^l$ are covered by the graph patterns in $\mathcal{P}^l$.

Intuitively, an explanation view $\mathcal{G}_{\mathcal{V}}^l$ provides a two-tier interpretation of GNNs in terms of a specific label l of interest. The "lower-tier" explanation subgraph explains GNN w.r.t. a label of interest with consistent and counterfactual properties. The "higher-tier" patterns serve as a concise summary to enable easy accessing, querying, and inspection of the classification and explanation results. Prior works verify the need and effectiveness of two-level explanation structures: a higher-level example, global "concept", or "prototype" patterns of each class (similar to our higher-tier patterns) for effective querying and summary of lower level detailed explanations [6, 13, 57].

Example 2.1. For a pretrained GNN model $\mathcal{M}$ in Example 1.1, we observe (and experimentally verified) the following. (1) For the label group mutagen $\{G_1, G_2\}$ classified by the GNN $\mathcal{M}$, an explanation view $\mathcal{G}_{\mathcal{V}}^{mutagen} = (\mathcal{P}^{mutagen}, \mathcal{G}_s^{mutagen})$. (a) $\mathcal{G}_s^{mutagen} = \{G_{s1}, G_{s2}\}$ contains two explanation subgraphs G_{s1} of G_1 and G_{s2} of G_2. $\mathcal{M}$ will incorrectly classify the remaining fraction of G_1 (resp. G_2) obtained by removing G_{s1} (resp. G_{s2}) as nonmutagen. (b) $\mathcal{P}^{mutagen} = \{P_{11}, P_{12}\}$ contains two graph patterns that concisely summarize the structural information of all the explanation subgraphs in $\mathcal{G}_s^{mutagen}$, with all the nodes covered by $\mathcal{P}^{mutagen}$. (2) Similarly, for the label nonmutagens, an explanation view $\mathcal{G}_{\mathcal{V}}^{nonmutagen}$ contains explanation subgraph set $\mathcal{G}_s^{nonmutagen}$ as $\{G_{s3}, G_{s4}\}$, and a set of patterns $\mathcal{P}^{nonmutagen} = \{P_{21}, P_{22}\}$.

Consider adding two more graphs $\{G_5, G_6\}$ in Figure 2 to mutagen group classified by $\mathcal{M}$. An explanation view of $\{G_5, G_6\}$ for $\mathcal{M}$ with label mutagen is illustrated on the right side, which contains two new explanation subgraphs G_{s5} and G_{s6}, and a pattern set $\{P_{31}, P_{32}, P_{33}\}$. Ideally, one wants to efficiently maintain the explanation view $\mathcal{G}_{\mathcal{V}}^{mutagen}$ by properly enlarging $\mathcal{P}^{mutagen}$ and $\mathcal{G}_s^{mutagen}$ only when necessary. For example, it suffices to keep only P_{11} or P_{32}, and P_{12} or P_{31}, in $\mathcal{P}^{mutagen}$.

Given a set of interested labels[2] Ł, and graph database $\mathcal{G}$ where each graph $G \in \mathcal{G}$ is assigned one of the labels $l \in$ Ł, we are interested in generating and maintaining a set of |Ł| explanation views $\mathcal{G}_{\mathcal{V}}^Ł = \{\mathcal{G}_{\mathcal{V}}^l | l \in$ Ł$\}$, one for each label group. Note that a label group may have multiple potential explanation views. We will elucidate the quality measures to determine the optimal explanation views for a given label group, and introduce algorithms to compute and maintain explanation views in the following sections.

3 VIEW-BASED EXPLANATION

Given a graph database $\mathcal{G}$ and a GNN $\mathcal{M}$, there naturally exist multiple explanation views for the classification results of $\mathcal{M}$ over $\mathcal{G}$. *How to measure their "goodness"?* We start with desirable

---

[1]We remark that G_s may be disconnected; for this case, each disconnected component can be considered as an explanation subgraph "corresponding" to G.

[2]We abuse the notation Ł and let it denote a set of user's interested labels.

properties and introduce quality measurements (§3.1), followed by the problem formulation (§3.2) and an analysis of properties and complexity (§3.3).

3.1 Quality Measures

Explainability. Our first measure quantifies how well the "lower tier" explanation subgraphs of explanation views interpret a GNN $\mathcal{M}$, naturally under the *influence maximization* principle: An explanation view has better explainability if its explanation subgraphs involve more nodes with features that can maximize their influence via a random walk-based message passing process (following Eq. 1). For GNNs that learn and infer via feature propagation, this principle has been consistently adopted to understand the accuracy of GNNs [56, 74] and their robustness [4], i.e., the likelihood the labels are changed when the features of such nodes are changed.

Given a label group $\mathcal{G}^l = \{G_1, \ldots, G_n\}$ and k-layer GNN $\mathcal{M}$, the *explainability* of an explanation view $\mathcal{G}^l_{\mathcal{V}} = (\mathcal{P}^l, \mathcal{G}^l_s)$ for $\mathcal{M}$ over $\mathcal{G}^l$ is quantified as:

$$f(\mathcal{G}^l_{\mathcal{V}}) = \sum_{G_{si} \in \mathcal{G}^l_s} \frac{I(V_{si}) + \gamma D(V_{si})}{|V_i|} \tag{2}$$

where (1) V_{si} is the node set of an explanation subgraph G_{si} of G ($G_{si} \in \mathcal{G}^l_s$, and $G_i \in \mathcal{G}$ for $i \in [1, n]$), and V_i is the node set of G_i ($V_{si} \subseteq V_i$); (2) $I(V_{si})$ is a function that quantifies the "influence" of the features of the node set $\mathcal{V}_s$ via feature propagation in the inference process of $\mathcal{M}$, and (3) $D(V_{si})$ is a diversity measure to capture influence maximization. Here a weight $\gamma \in [0, 1]$ is introduced to balance between feature influence and diversity.

We next introduce the two functions $I(\cdot)$ and $D(\cdot)$.

Feature Influence. Following feature sensitivity and influence analysis in GNNs [56, 74], we introduce an *influence* score. Given a graph G with node set V, the influence of a node u on another node v at the k-layer propagation is defined as the L1-norm of the expected Jacobian matrix [56]:

$$I_1(v, u) = \left\| \mathbb{E}[\partial X_v^k / \partial X_u^0] \right\|_1 \tag{3}$$

Intuitively, $I_1(v, u)$ quantifies how "sensitive" the representation X_v^k of a node v at the k-th layer of $\mathcal{M}$ is, upon changes of the representation X_u^0 at the input layer of $\mathcal{M}$ for a given connected node u; in other words, how "influential" u to v is via feature propagation.

Given a targeted node v, the influence score of a node $u \in V$ to v can be normalized as

$$I_2(u, v) = \frac{I_1(v, u)}{\sum_{w \in V} I_1(v, w)} \tag{4}$$

Given a threshold θ and a set of nodes $V_s \subseteq V$, we say that a node v is *influenced* by V_s if there exists a node $u \in V_s$, such that $I_2(u, v) \geq \theta$. The influence score of V_s, denoted as $I(V_s)$, is in turn defined as the size of nodes influenced by V_s, i.e.,

$$I(V_s) = |\{v | I_2(u, v) \geq \theta, u \in V_s, v \in V\}| \tag{5}$$

Neighborhood Diversity. The second function aggregates a diversity measure among the neighboring nodes influenced by the explanation subgraphs via feature propagation. Recall that the node representation of v at the output layer (the k-th layer) of the GNN $\mathcal{M}$ is X_v^k. Let $r(v, d)$ be the set of nodes in V such that for each node $v' \in r(v, d)$, the distance $d(X_v^k, X_{v'}^k)$ between nodes v and v' is bounded by a threshold r, i.e., $r(v, d) = \{v' | d(X_v^k, X_{v'}^k) \leq r, v, v' \in V\}$.

The function $D(V_s)$ quantifies a *neighborhood diversity* as size of the union of $r(u, d)$ for each node u influenced by V_s, i.e.,

$$D(V_s) = \left| \bigcup_{v : I_2(V_s, u, v) \geq \theta} r(v, d) \right| \tag{6}$$

Here the distance function $d(\cdot)$ can be any embedding distance measure, such as the normalized Euclidean distance.

Putting these together, an explanation view with higher explainability favors explanation subgraphs that **(1)** have greater feature influence following feature propagation process, and **(2)** influence more nodes with larger neighborhood diversity.

Coverage. Besides "lower-tier" explainability, we also expect the "higher-tier" patterns of an explanation view to *cover* a desirable amount of nodes for each label group of interests. Better still, such coverage constraints should be explicitly configurable by users. These coverage constraints become especially valuable when conducting label-specific analyses on multiple labeled groups [38, 69].

Given a label group $\mathcal{G}^l = \{G_1, \ldots G_n\}$, and its node set $\mathcal{V}^l = \bigcup_{G_i \in \mathcal{G}^l} V_i$, a coverage constraint is a range $[b_l, u_l]$, where $0 \leq b_l \leq u_l \leq |\mathcal{V}^l|$. We say that an explanation view $\mathcal{G}^l_{\mathcal{V}} = (\mathcal{P}^l, \mathcal{G}^l_s)$ *properly covers* the label group $\mathcal{G}^l$ if the explanation subgraphs $\mathcal{G}^l_s$ contain in total n nodes from $\mathcal{V}^l$ where $n \in [b_l, u_l]$. Note that by definition of graph views, $\mathcal{P}^l$ also covers all the nodes from $\mathcal{G}^l_s$.

3.2 Explanation View Generation Problem

Configuration. A *configuration* C specifies the following parameters: (1) a pair of thresholds (θ, r) to determine the influence and diversity scores in explainability measure; and (2) a set of coverage constraints $\{[b_l, u_l]\}$ for each class label $l \in Ł$.

We now formulate the problem of *Explanation View Generation*.

PROBLEM 1. *Given a graph database $\mathcal{G}$, a set of interested labels $Ł$ s.t. $|Ł| = t$, a GNN $\mathcal{M}$, and a configuration C, the* explanation view generation problem, *denoted as* EVG, *is to compute a set of graph views $\mathcal{G}_{\mathcal{V}} = \{\mathcal{G}^{l_1}_{\mathcal{V}}, \ldots \mathcal{G}^{l_t}_{\mathcal{V}}\}$, such that ($i \in [1, t]$):*

- *Each graph view $\mathcal{G}^{l_i}_{\mathcal{V}} = (\mathcal{P}^{l_i}, \mathcal{G}^{l_i}_s) \in \mathcal{G}_{\mathcal{V}}$ is an explanation view of $\mathcal{G}$ for $\mathcal{M}$ w.r.t. $l_i \in Ł$;*
- *Each $\mathcal{G}^{l_i}_{\mathcal{V}}$ properly covers the label group $\mathcal{G}^{l_i}$; and*
- *$\mathcal{G}_{\mathcal{V}}$ maximizes an aggregated explainability, i.e.,*

$$\mathcal{G}_{\mathcal{V}} = \arg\max \sum_{\mathcal{G}^{l_i}_{\mathcal{V}} \in \mathcal{G}_{\mathcal{V}}} f(\mathcal{G}^{l_i}_{\mathcal{V}}) \tag{7}$$

That is, we are interested in generating a set of explanation views which maximizes the explainability and simultaneously properly covers $\mathcal{G}$ w.r.t. the configuration for each labeled group.

3.3 Hardness and Properties

To understand the hardness and feasibility of generating explanation views for GNNs, we study several fundamental issues and properties. Our results are established for a *fixed* GNN model $\mathcal{M}$. We follow the convention in cost analysis of GNNs [21], and say that $\mathcal{M}$ is "fixed" if it is given, pretrained (thus, its architecture and weights no longer change), and incurs an inference cost in polynomial time (PTIME).

View Verification. To understand the hardness of EVG, we first investigate a "building block" decision problem, notably, *view verification*. Given $\mathcal{G}, C, Ł$, a fixed GNN $\mathcal{M}$, and a two-tier structure $\mathcal{G}_{\mathcal{V}} = (\mathcal{P}, \mathcal{G}_s)$ with a pattern set $\mathcal{P}$ and a set of subgraphs $\mathcal{G}_s$ of the graphs from $\mathcal{G}$, it verifies if

$\mathcal{G}_\mathcal{V}$ satisfies three constraints simultaneously: (**C1**): it is a graph view of $\mathcal{G}$, (**C2**): if so, if it is an explanation view of the label group $\mathcal{G}^l = \{G\}$, where $\mathcal{M}(G) = l$; and (**C3**): if so, if it properly covers $\mathcal{G}^l$ under the coverage constraint in C.

The hardness of verification provides the lower bound results for EVG, and its solution will be used as a primitive operator in GVEX view generation framework (see §4). And then we present the following result.

LEMMA 3.1. *Given a graph database* $\mathcal{G}$, *configuration* C, *and a two-tier structure* $(\mathcal{P}, \mathcal{G}_s)$, *the view verification problem is* **NP**-*complete when the* GNN $\mathcal{M}$ *is fixed.*

Proof sketch: It is not hard to verify that view verification is **NP**-hard, given that it requires subgraph isomorphism tests alone to verify constraint **C1**, which is known to be **NP**-hard [17]. We next outline an **NP** algorithm for the verification problem. It performs a three-step verification below. (1) For **C1**, it guesses a finite number of matching functions in PTIME (for patterns $\mathcal{P}$ and $\mathcal{G}$ with bounded size), and verifies if the patterns induce accordingly $\mathcal{G}_s$ via the matching functions in PTIME. If so, $\mathcal{G}_\mathcal{V}$ is a graph view. (2) To check **C2**, for each graph $G \in \mathcal{G}$ and its corresponding subgraphs $G_s \in \mathcal{G}_s$, it applies $\mathcal{M}$ to verify if $\mathcal{M}(G_s) = l$ and $\mathcal{M}(G \setminus G_s) \neq l$. If so, $\mathcal{G}_\mathcal{V}$ is an explanation view for $\mathcal{G}$. For a fixed GNN $\mathcal{M}$, it takes PTIME to do the inference. (3) It takes PTIME to verify the coverage given that subgraph isomorphism tests have been performed in steps (1) and (2). These verify the upper bound of view verification.

Hardness of EVG. Given a threshold h, the decision problem of EVG is to determine if there exists a set of explanation views $\mathcal{G}_\mathcal{V}$ for GNN $\mathcal{M}$ with explainability at least h under the constraints in C. We present a hardness result below for EVG.

THEOREM 3.2. *For a fixed* GNN $\mathcal{M}$, *EVG is (1)* Σ_P^2-*complete, and (2) remains* **NP**-*hard even when* $\mathcal{G}$ *has no edges.*

Here a problem is in Σ_P^2 if an **NP** algorithm exists to solve it with an **NP** oracle. Theorem 3.2 verifies that it is beyond **NP** to generate explanation views under coverage constraints, thus the general EVG problem is hard even for fixed GNNs. We outline the hardness analysis below and present the detailed proof in the appendix.

Proof sketch: (1) EVG is solvable in Σ_P^2 since we can devise an **NP** oracle for view verification by guessesing a set of two-tier view structures $\mathcal{G}_\mathcal{V} = \{(\mathcal{P}, \mathcal{G}_s)_i\}$ ($i \in [1, |Ł|]$) and calling the **NP** algorithm in the proof of Lemma 3.1 $O(|Ł||\mathcal{P}||\mathcal{G}|)$ times to check the fulfillment of the three constraints. If so, it then computes $f(\mathcal{G}_\mathcal{V}^l)$ and checks if $f(\mathcal{G}_\mathcal{V}^l) \geq h$ in PTIME. (2) To see that EVG is Σ_P^2-hard, we construct a reduction from graph satisfiability, a known Σ_P^2-complete problem [43]. (3) To see Theorem 3.2(2), we consider a special case of EVG. Let $\mathcal{G}$ contains two single graphs G_1 and G_2, each has no edge. For such a case, we prove that EVG remains to be **NP**-hard through a reduction from the red-blue set cover problem [8], which is **NP**-complete. This verifies the hardness of EVG for identifying explanation with coverage requirement alone, as in such case, subgraph isomorphism test is no longer intractable.

While Theorem 3.2 tells us that EVG is in general hard, we next show its properties that indicate feasible algorithms with provable quality guarantees in practice.

Monotone Submodularity. We first show that the explainability $f(\mathcal{G}_\mathcal{V})$ of an explanation view $\mathcal{G}_\mathcal{V}$ is essentially a *monotone submodular* set function [7], determined by the nodes from its explanation subgraphs. Clearly, $f(\mathcal{G}_\mathcal{V})$ is non-negative. Denote the set of nodes from $\mathcal{G}_\mathcal{V}^l$ as V_s, with V_s ranges over the node set of G_s in $\mathcal{G}_s^l$.

LEMMA 3.3. *Given* $\mathcal{G}$, *Ł*, *C*, *and a fixed* GNN $\mathcal{M}$, $f(\mathcal{G}_\mathcal{V})$ *is a monotone submodular function.*

Proof sketch: We first show that the monotonicity and submodularity of $f(\cdot)$ depend on the two components $I(\cdot)$ and $D(\cdot)$. Then we show that enlarging the node set will never downgrade the feature influence, thus $I(\cdot)$ is monotonic. Next we systematically discuss the marginal gain of $I(\cdot)$ for any set $V_{s''} \subseteq V_{s'}$ and any node $u \notin V_{s'}$ under several cases, leading to a conclusion that $|\mathsf{Inf}(V_{s''} \cup \{u\})| - |\mathsf{Inf}(V_{s''})| \geq |\mathsf{Inf}(V_{s'} \cup \{u\})| - |\mathsf{Inf}(V_{s'})|$. Finally, we show that the similar properties of $D(\cdot)$ can be analyzed in the same manner. The complete proof is in the appendix.

We next present an algorithm framework, denoted as **GVEX**, to solve the EVG problem. We show that there exists feasible approximations for EVG in §4, and then introduce an efficient algorithm to maintain explanation views in §5.

4 GENERATING EXPLANATION VIEWS

Our main results below show that there exist feasible algorithms to generate explanation views with guarantees on both explainability and coverage constraints, for GNN-based graph classification.

THEOREM 4.1. *Given a configuration C, graph database $\mathcal{G}$, and a k-layer GNN $\mathcal{M}$ over label set Ł, there is a $\frac{1}{2}$-approximate algorithm for generating explanation views, and takes $O(|\mathcal{G}||V_m|^3 + |\mathcal{G}||V_m||Ł|k \cdot C.u_l(dD + D^2) + N(N + T))$ time.*

Here, $|\mathcal{G}|$ is the number of graphs in $\mathcal{G}$; V_m refers to the largest node set of a graph in $\mathcal{G}$, d and D are the average degree and the number of features per node, and N and T are the total number of verified patterns and the cost for single isomorphism test, respectively.

We start by presenting an approximation algorithm that generates an explanation view for a single label $l \in Ł$ and a single graph $G \in \mathcal{G}^l$. Our general approximation scheme calls this algorithm for each graph $G \in \mathcal{G}^l$ to assemble an explanation view $\mathcal{G}_{\mathcal{V}}^l$, and then returns a set of explanation views $\mathcal{G}_{\mathcal{V}}$ as $\bigcup_{l \in Ł} \mathcal{G}_{\mathcal{V}}^l$.

"Explain-and-Summarize". Our general idea is to follow a two-step "explain-and-summarize" strategy. (1) In the "explain" stage, the algorithm selects high-quality nodes to induce "lower-tier" explanation subgraphs for $\mathcal{M}$ that can maximize the explainability score, and meanwhile, ensures the coverage constraints in the configuration C. (2) The "summarize" stage produces, as "higher-tier" structure, a set of graph patterns that ensures to cover the nodes of the explanation subgraphs. The computed components are then assembled to yield the desired explanation views. The output of the two stages captures explainability and provides queryable property, respectively.

To ensure the quality guarantee and efficiency, the algorithm adopts several primitive operators, which are described below.

Verifiers. The verifiers are efficient operators that implement the view verification to check the constraints **C1**-**C3** as specified by configuration C (see the proof of Lemma 3.1), whenever a two-tier structure $(\mathcal{P}, \mathcal{G}_s)$ is in place. GVEX calls two primitive verifiers:

- a GNN inference operator EVerify, which efficiently infers the label of a subgraph G_s of G and its counterpart $G \setminus G_s$ with $\mathcal{M}$ (constraint **C2**); and
- a pattern matching operator PMatch, that performs fast node-induced subgraph isomorphism and checks whether the nodes in explanation subgraphs are covered by patterns (constraint **C1**), and are also properly covered (constraint **C3**).

Since the view verification problem is **NP**-complete, we approach it by addressing constraints using two efficient primitive verifiers. It allows us to offer a feasible solution and establishes lower bound results for EVG. In practice, they can be supported by invoking established solutions, e.g., parallel GNN inference [19, 31] and subgraph pattern matching [23, 46], respectively.

Algorithm 1 Algorithm ApproxGVEX (for a single graph G)

Input: A graph G, a GNN $\mathcal{M}$, a label l, a configuration C;
Output: an explanation view $\mathcal{G}_{\mathcal{V}}^l$ for G and l.

1: set $V_S := \emptyset$; set $V_u := \emptyset$; set $\mathcal{G}_s^l := \emptyset$; set $\mathcal{G}_{\mathcal{V}}^l := \emptyset$; set $\mathcal{P}:=\emptyset$;
2: Invoke EVerify to precompute Jacobian Matrix M_I of G;
   /* *explanation phase* */
3: **while** $|V_S| < C.u_l$ **and** $V\backslash V_S \neq \emptyset$ **do**
4:    **for** $v \in V\backslash V_S$ **do**
5:       **if** VpExtend $(v, V_S, G, \mathcal{G}_s^l, C, \mathcal{M})$ **then**
6:          $V_u := V_u \cup \{v\}$;
7:    $v^* := \text{argmax}_{v' \in V_u}(f(V_S \cup v') - f(V_S))$;
8:    $V_S := V_S \cup \{v^*\}$;
9:    extend $\mathcal{G}_s^l$ with the selected node v^*;
   /* *use candidate set V_u to satisfy lower bound requirement* */
10: **while** $|V_S| < C.b_l$ **and** $V_u \neq \emptyset$ **do**
11:    **for** $v' \in V_u$ **do**
12:       **if** VpExtend $(v', V_S, G, \mathcal{G}_s^l, C, \mathcal{M})$ **then**
13:          $v^* := \text{argmax}_{v' \in V_u}(f(V_S \cup v') - f(V_S))$;
14:          $V_S := V_S \cup \{v^*\}$;
15:          extend $\mathcal{G}_s^l$ with the selected node v^*;
   /* *no "large enough" explanation that satisfy lower bound* */
16:    **if** $V_u = \emptyset$ **and** $|V_S| < C.b_l$ **then**
17:       **return** $\emptyset$;
   /* *summary phase* */
18: $\mathcal{G}_{\mathcal{V}}^l := \text{Psum} (\mathcal{G}_s^l, V_S)$;
19: **return** $\mathcal{G}_{\mathcal{V}}^l$;

Pattern generators. We use a second operator PGen to extract a set of pattern candidates to be verified by PMatch, from a set of explanation subgraphs. The operator exploits minimum description length (MDL) principle and conducts a constrained graph pattern mining process. It can be implemented by invoking scalable pattern mining algorithms, e.g., [59]. Advanced mining algorithms developed in the future can be used to enhance the PGen method further.

Algorithm. The algorithm, denoted as ApproxGVEX (Algorithm 1), computes an explanation view $\mathcal{G}_{\mathcal{V}}^l$ for a label $l \in \text{Ł}$ and a graph G.

Initialization (lines 1-2). ApproxGVEX initializes and maintains the following auxiliary structures (i.e., initialized globally once, and not re-initialized for each graph): (1) two node-sets V_u and V_S, to store the candidate nodes and the selected ones that contribute to inducing explanation subgraphs, respectively; (2) a set $\mathcal{G}_s^l$ of explanation subgraphs to be summarized, and the explanation view $\mathcal{G}_{\mathcal{V}}^l$. In addition, it also pre-computes the Jacobian matrix M_I with the operator EVerify. Note that this once-for-all inference also prepares node representations that are needed to compute $I(\cdot)$ and $D(\cdot)$.

Explanation phase (lines 3-10). In this phase, ApproxGVEX dynamically expands a set of selected nodes V_S with high influence scores to construct explanation subgraphs. (1) It first checks if a new node in $\mathcal{V} \setminus V_S$ can contribute to "extend" an existing explanation subgraph in its original graph $G \in \mathcal{G}$, by invoking procedure VpExtend (line 7, to be discussed). (2) Upon the enlargement of V_u, it adopts a greedy selection strategy to iteratively choose the node v^* from V_u that can maximize
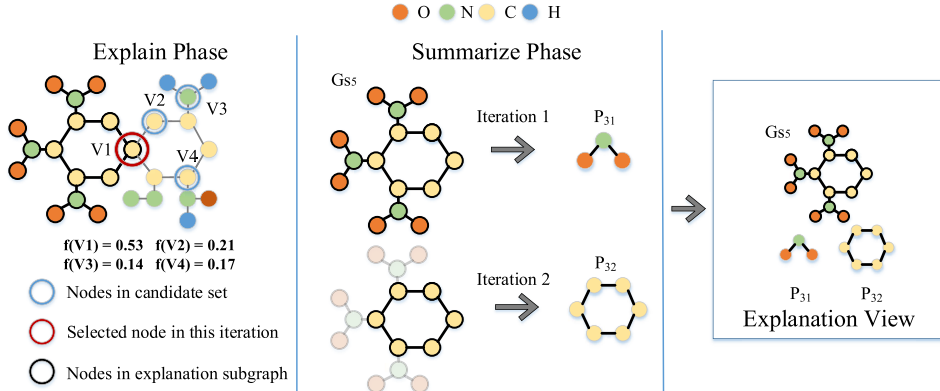
Fig. 3. "Explain-and-Summarize": an illustration

the marginal gain (line 9). It then extends V_S with v^*, and updates the current set of explanation subgraphs by including v^* and its induced edges in G until finish condition (line 3). ApproxGVEX then takes care of the lower bound requirement (lines 10-17). If $\mathcal{G}_s^l$ contains too few nodes V_S to satisfy the lower bound requirement $C.b_l$ (line 10), it repeats the greedy selection from the candidate set V_u, until $\mathcal{G}_s^l$ grows to desired size or no candidate node is available (line 10). If all candidates are processed and $\mathcal{G}_s^l$ is still small, ApproxGVEX returns $\emptyset$ (lines 16-17).

Summary phase (line 18). In this phase, ApproxGVEX invokes procedure Psum to construct patterns that cover V_S with a small number of patterns. It then constructs and returns $\mathcal{G}_{\mathcal{V}}^l$.

   We next present the details of the procedures VpExtend and Psum.

Procedure 2 Procedure VpExtend $(v, V_S, G, G_s, C, \mathcal{M})$

 1: Update explanation subgraph G_s with v to G_t;
    /*invokes EVerify *to verify constraint **C2** ("View verification"; § 3.3)*/
 2: **if** $\mathcal{M}(G_t) \neq \mathcal{M}(G)$ **or** $\mathcal{M}(G \backslash G_t) = \mathcal{M}(G)$ **then**
 3:     **return** *false*
 4: set $V_t := V_S \cup \{v\}$;
 5: **if** $|V_t| \geq C.u_l$ **then**
 6:     **return** *false*;
 7: **return** *true*;

Procedure VpExtend. The procedure VpExtend implements the view verification algorithm (see §3). It invokes the two verifier operators to determine if the explanation subgraphs, in particular, the nodes V_S that are used to induce them, can be "extended". It first constructs an explanation subgraph by augmenting the current fraction that belongs to $\mathcal{G}_s^l$ with the node v to be verified, and follows the verification process to check the invariant conditions, i.e., consistency, counterfactual explanation, and coverage conditions.

   Example 4.2. Figure 3 illustrates the "Explain-and-Summarize" process, with a configuration $C = (0.14, 2, (0, 15))$. (1) In the explanation phase, ApproxGVEX identifies four candidate nodes $\{v_1, v_2, v_3, v_4\}$, which pass the verification in VpExtend. These nodes are stored in V_u. (2) It then greedily selects the node v_1 with the highest gain on explainability for $\mathcal{G}_s^l$ (with a score 0.53 in our experiment). This repeats until V_u are processed and an explanation subgraph is induced as G_{s5}. Since the upper bound $u_l = 15$ is reached, G_{s5} is returned as an explanation subgraph.

Procedure Psum. Given the explanation subgraphs $\mathcal{G}_s^l$ induced from explanation phase, procedure Psum computes a set of "higher-tier" patterns $\mathcal{P}$ to cover the nodes of $\mathcal{G}_s^l$. Meanwhile, it is desirable for $\mathcal{P}$ to cover the edge set of $\mathcal{G}_s^l$ as much as possible. Given a pattern $P \in \mathcal{P}$ and graphs $\mathcal{G}_s^l$ with node set V_S and edge set E_S, we denote the nodes and edges in $\mathcal{G}_s^l$ it covers as P_{V_S} and P_{E_S}, respectively. Let each P be "penalized" by a normalized weight (as the Jaccard distance) between E_S and P_{E_S}, i.e., $w(P) = 1 - \frac{|P_{E_S}|}{|E_S|}$ (note $P_{E_S} \subseteq E_S$). The above requirements can be further formulated as an optimization problem:

- **Input**: explanation subgraphs $\mathcal{G}_s^l$;
- **Output**: a pattern set $\mathcal{P}^l$, such that (1) $\bigcup_{P \in \mathcal{P}^l}(P_{V_S}) = V_S$ and (2) $\mathcal{P}^l = \arg\min \sum_{P \in \mathcal{P}^l} w(P)$.

The procedure Psum solves the above problem by conducting a constrained pattern mining on explanation subgraphs $\mathcal{G}_s^l$. It invokes operator PGen to iteratively generate a set of pattern candidates (line 3), and subsequently adopts a greedy strategy to dynamically select a pattern P^* that maximizes a gain ascertained by covered nodes $\mathcal{P}_{V_S}^*$ in V_S with the smallest weight. $\mathcal{P}^l$ is enlarged with $\mathcal{P}^*$ accordingly. Post the selection of the currently optimal patterns, the matched nodes in V_S are reduced; and the weights of the patterns are updated accordingly. This allows us to gradually acquire the final explanation view and reduce the edges "missed" by $\mathcal{P}^l$.

LEMMA 4.3. *For a given set of explanation subgraphs $\mathcal{G}_s^l$, procedure* Psum *is an H_{u_l}-approximation of optimal $\mathcal{P}^l$ that ensures node coverage (hence satisfies coverage constraint in C). Here, $H_{u_l} = \sum_{i \in [1, C.u_l]} \frac{1}{i}$ is the u_l-th Harmonic number ($C.u_l \geq 1$).*

The quality guarantee can be verified by performing an approximate preserving reduction from the optimization problem to the minimum weighted set cover problem, for which a greedy selection strategy ensures an H_d-approximation with d the largest subset size [2], which is in turn bounded by $C.u_l$ for the patterns over node-induced subgraphs $\mathcal{G}_s^l$. We present the detailed analysis in the appendix.

Example 4.4. Continuing Example 4.2, given G_{s_5}, Psum generates a small set of 2 pattern candidates: P_{31} and P_{32}. It finds that P_{31} covers 9 nodes in G_{s5}, and specifically, capturing the presence of three nitro groups. Consequently, P_{31} is selected as the best pattern. The nodes already covered by P_{31} are masked, and a next pattern, P_{32} (carbon ring), is chosen as the second pattern that further covers 6 nodes in the remaining part. The two patterns properly cover all nodes of G_{s5}, with a small number (3) of edges uncovered. By incorporating G_{s5} with a pattern set $\mathcal{P} = \{P_{31}, P_{32}\}$, an explanation view $\mathcal{G}_{\mathcal{V}}^l$ is constructed as $(\mathcal{P}, G_{s5})$.

Correctness & Approximability. Algorithm ApproxGVEX terminates when: all nodes in V are processed ($V \setminus V_S = \emptyset$), or all candidates in V_u are exhausted (V_u is $\emptyset$). When it terminates with a non-empty $\mathcal{G}_s^l$, it correctly ensures that $\mathcal{G}_s^l$ is an explanation subgraph, as guarded by the verification of the three constraints **C1-C3** in view verification (by invoking procedures VpExtend and Psum).

To see the approximation guarantee, observe that ApproxGVEX generates $\mathcal{G}_s^l$ by carefully constructing V_S that satisfies the coverage constraint ($|V_S| \in [b_l, u_l]$). Given Lemma 3.3, it essentially solves EVG as a monotone submodular maximization problem under a range cardinality constraint. This allows us to reduce EVG to a fair submodular maximization problem [14]. The latter chooses a node set that maximizes a monotone submodular function under ranged coverage constraint (which is set as ($[C.b_l, C.u_l]$ in our case). The $\frac{1}{2}$-approximation [14] carries over for EVG, as ApproxGVEX carefully selects nodes with two invariants: (1) whenever $|V_S| \leq C.u_l$, it improves explainability of $\mathcal{G}_s^l$ via greedy strategy that ensures $\frac{1}{2}$-approximation by submodular maximization under metroid constraints [9], and (2) if $|V_S| \leq C.b_l$, it continues enlarging $\mathcal{G}_s^l$ with V_u that gathers "back up" nodes, this does not hurt the guarantee on explainability due to its *monotonic non-decreasing* property.

Algorithm 3 Algorithm StreamGVEX (for a single graph G)

Input: a graph G with label l, a GNN $\mathcal{M}$, a configuration C;
Output: An explanation view $\mathcal{G}_\mathcal{V}^l$;
1: set $V_S := \emptyset$; set $\mathcal{G}_\mathcal{V}^l := \emptyset$; set $\mathcal{P}_c := \emptyset$; set $V_u := \emptyset$;
2: **for** each arriving node $v \in V$ (as a node stream) **do**
3:    invoke IncEVerify to update Jacobian Matrix;
4:    $w(v) := f(V_S \cup \{v\}) - f(V_S)$;
5:    $V_u := V_u \cup \{v\}$;
6:    **if** VpExtend $(v, V_S, G, G_s, C, \mathcal{M})$ **then**
7:       $V_S :=$ IncUpdateVS (v, V_S, V, G, G_s);
8:    **if** $v \in V_S$ **then**
9:       $\mathcal{P}_c :=$ IncUpdateP $(v, V_S, \mathcal{P}_c)$;
10: use set V_u to update V_S to satisfy lower bound constraint $C.b_l$;
11: **return** $\mathcal{G}_s^l$ as $(\mathcal{P}, \mathcal{G}_s)$;

Time Cost. ApproxGVEX incurs a one-time cost in $O(|V|^3)$ to compute Jacobian matrix (line 2). It takes at most $|V|$ rounds in generating V_S. For a fixed GNN with k-layers, a full inference takes $O(k|V_S|(dD + D^2))$ [75], where d and D refer to the average degree of G_s^l and the number of features per node. Thus in each round, VpExtend takes $O(k \cdot C.u_l(dD + D^2))$ time to verify if G_s^l remains to be an explanation subgraph. The total time cost of Psum is $O(N * T + N^2)$, where N is the number of verified patterns (each with at most $C.u_l$ nodes) from G_s^l, and T is the time cost of PMatch. Hence the total cost is $O(|V|^3 + k \cdot C.u_l(dD + D^2) + N(N + T))$. In practice, d and D are small, and N and T are also small due to bounded pattern and graph size.

To generate $\mathcal{G}_\mathcal{V}$ over $\mathcal{G}$ and Ł, one invokes ApproxGVEX at most $|\mathcal{G}|$ times. The overall time cost is: $O(|\mathcal{G}||V_m|^3 + |\mathcal{G}||V_m||Ł|k \cdot C.u_l(dD + D^2) + N(N + T))$, with V_m the largest node set of a graph in $\mathcal{G}$, and the rest terms scale to their counterparts for $\mathcal{G}$.

5 FAST STREAMING-BASED ALGORITHM

Algorithm ApproxGVEX requires the generation of all explanation subgraphs to complete the generation of explanation views. As such, GNN inference or pattern generation alone can be major bottlenecks when G is large. Moreover, users may also want to interrupt view generation to investigate and ad-hocly query for specific explanation structures. In response, we next outline an algorithm to *incrementally* maintain explanation views as it scans over G as a stream of nodes.

THEOREM 5.1. *Given a configuration C, graph database $\mathcal{G}$, GNN $\mathcal{M}$, there is an online algorithm that maintains explanation views with a $\frac{1}{4}$-approximation.*

The above approximation ratio holds for an optimal explanation view on the "seen" fraction of $\mathcal{G}$, thus is a weaker form of guarantee; yet this provides a pragmatic solution for large $\mathcal{G}$.

Our idea is to treat the node set of G as a stream, and incrementalize the update of "lower-tier" explanation graph G_s^l and *accordingly* the "affected" higher-tier patterns $\mathcal{P}$, to reduce unnecessary verification. To this end, it uses the following procedures: (1) IncEVerify and IncPMatch: Upon the arrival of a node v, IncEVerify only updates the feature influence $I_1(., v)$, diversity $D(v)$, and updates $I(V_S \cup \{v\})$ and $D(V_S \cup \{v\})$ incrementally; IncPMatch invokes fast incremental and streaming subgraph matching algorithms, e.g., [15, 33] to check graph views, explanation views, and proper coverage. (2) IncPGen: unlike PGen, it takes as input a small subgraph induced by the r-hop neighbors of v (where r is specified in C for neighborhood influence), and only generates new patterns $\Delta \mathcal{P}$ not in $\mathcal{P}^l$, to be verified by IncPMatch; (3) IncUpdateP and IncUpdateVS maintain $\mathcal{P}^l$
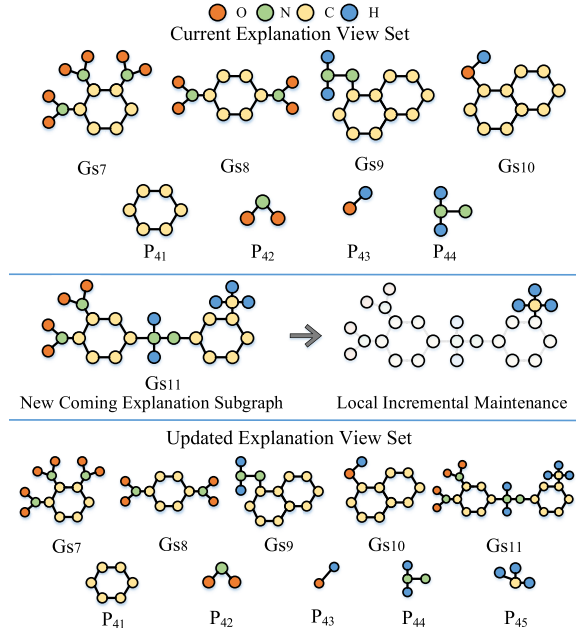
Fig. 4. Incremental generation of explanation views

and G_s^l respectively, with a space-efficient "swapping" strategy (to be discussed) to dynamically decide whether to replace patterns.

Algorithm. The algorithm, denoted as StreamGVEX, is outlined in Algorithm 3. Upon the arrival of a node v, it invokes IncEVerify to maintain the Jacobian matrix, updates the marginal gain, and enlarges the candidate set V_u. It then tests the extendability of V_S, and invokes IncUpdateVS and IncUpdateP to update $\mathcal{P}^l$ and G_s^l respectively. The "post processing" is similar as its counterpart in ApproxGVEX (line 10) ensures the lower bound.

Local Incremental Update. IncUpdateVS maintains V_S as a node cache of size up to $C.u_l$. For a node v that passes extendable test (line 6), it consults a greedy swapping strategy to decide whether to replace a node $v' \in V_S$ with v or reject v, and put the node v' into V_u. Specifically, it performs a case analysis: (a) if $|V_S| < C.u_l$, it simply adds v to V_S; (b) otherwise, if $\mathcal{P}^l$ already covers v, or v alone does not contribute new patterns to $\mathcal{P}^l$ ($\Delta \mathcal{P} = \emptyset$, as determined by IncPGen), it skips processing v, as this does not hurt the quality of the current explanation view; (b) otherwise, it chooses the node $v' \in V_S$ whose removal has the smallest "loss" of explainability score, and replaces v' with v only when such a replacement ensures a gain that is at least twice as much as the loss. In other words, the replacement does not hurt the original approximation ratio.

Upon the formation of new explanation subgraphs, IncUpdateP performs a similar case analysis, yet on patterns $\mathcal{P}^l$, and conducts a swapping strategy to ensure node coverage and small edge misses. We present the details of IncUpdateVS and IncUpdateP in the appendix.

Example 5.2. Figure 4 illustrates the maintenance of an explanation view with four explanation subgraphs ($\{G_{s7}, G_{s8}, G_{s9}, G_{s10}\}$ that are properly covered by four patterns $\{P_{41}, P_{42}, P_{43}, P_{44}\}$). Upon the processing of a new node, a newly induced explanation subgraph G_{s11} is to be processed. As existing patterns $\{P_{41}, P_{42}, P_{43}, P_{44}\}$ already cover a fraction of G_{s11}, StreamGVEX masks the nodes that are covered and proceeds to generate a new pattern P_{45} from G_{s11} to cover its remaining fraction. The explanation view is eventually enriched with G_{s11} and a new pattern P_{45}.

Analysis. The approximation guarantee of StreamGVEX comes from the $\frac{1}{4}$-approximation ensured by the streaming submodular maximization [14], as well as the online optimization of full coverage during the explanation generation. Specifically, its greedy local replacement strategy ensures an invariant that the selected nodes do not impact the $\frac{1}{4}$ approximation ratio. Online pattern generation does not affect the full coverage property, thus assuring quality. StreamGVEX offers the advantage of not requiring a comparison of information from all nodes each time, allowing anytime access of explanation views. As the processing is performed "one node at a time", the pattern generation is expedited, further enhancing its speed.

StreamGVEX does not require any prior node order. *(i)* It ensures "anytime" quality guarantees regardless of node orders (Theorem 5.1). *(ii)* Prioritizing some nodes may allow the early discovery of certain frequent patterns. IncUpdateP maintains $\mathcal{P}^l$ with a space-efficient "swapping" strategy to dynamically decide whether to replace patterns and nodes. Thus, the higher-tier patterns may vary slightly under different node orders, though a significant majority of the important patterns captured will be similar. *(iii)* Different node orders in StreamGVEX does not affect the worst case time cost.

Parallel Implementation. To generate $\mathcal{G}_V$ over $\mathcal{G}$ with multiple labels, one can readily apply a parallel scheme with $|\mathcal{G}|$ processes, each processes a node stream by invoking StreamGVEX. We present a detailed analysis in the appendix.

6 EXPERIMENTAL STUDY

We conduct an empirical evaluation of our solutions and existing approaches using both real-world and synthetic graph databases (Table 3). All methods are implemented in Python. The experiments are executed on a Ubuntu machine with one NVIDIA GeForce RTX 3090 GPU and 128G RAM on Intel(R) Xeon(R) CPU E5-2650 v4 @ 2.20GHz CPU. We employ multi-processing to demonstrate the parallelism of our algorithms. Our code and datasets are at [1].

Table 3. Dataset statistics. NF inidicates node features.

Dataset	Avg # Edges per graph	Avg # Nodes per graph	# NF per node	# Graphs	# Classes
MUTANGENICITY	31	30	14	4337	2
REEDIT-BINARY	996	430	-	2000	2
ENZYMES	62	33	3	600	6
MALNET-TINY	2860	1522	-	5000	5
PCQM4Mv2	31	15	9	3 746 619	3
PRODUCTS	5 728 239	1 184 330	100	1	47
SYNTHETIC	1 999 975	400 275	-	100	2

6.1 Experimental Setup

Datasets. (1) MUTAGENICITY (MUT**)** [32] is a molecular dataset for binary classification task. Each graph represents a chemical compound, where nodes are atoms and undirected edges denote bonds. The one-hot node feature indicates the atom type, e.g., carbon, oxygen. **(2) REDDIT-BINARY (**RED**)** [60] is a social network dataset comprising 2000 online discussion threads on Reddit. Nodes are users participating in a certain thread, while an edge denotes that a user responded to another. These graphs are labeled based on two types of user interactions, *question-answer* and *online-discussion*, in the threads. **(3) ENZYMES (**ENZ**)** [5] is a protein dataset, containing hundreds of undirected protein-protein interaction structures for up to six types of enzymes. One-hot node features indicate the type of protein. **(4) MALNET-TINY (**MAL**)** [18] is an ontology of malicious software function call graphs (FCGs). Each FCG captures calling relationships between functions within a program, with nodes representing functions and directed edges indicating inter-procedural calls. The individual

graph size in this dataset is considerably larger, posing additional challenges for identifying concise explanation substructures. **(5) PCQM4Mv2** (PCQ) [24] is a quantum chemistry dataset originally curated under the PubChemQC project. It provides molecules as the SMILES strings, from which 2D molecule undirected graphs (nodes are atoms and edges are chemical bonds) are constructed, where each node is associated with a 9-dimensional feature fingerprint. **(6) PRODUCTS** (PRO) [26] represents an Amazon product co-purchasing network and consists of an undirected, unweighted graph containing 2,449,029 nodes and 61,859,140 edges. The task is to predict the category of a product, where the 47 top-level categories are used as target labels. Originally it was designed for node classification and we transform this dataset for a graph classification task by sampling 400 subgraphs from the original graph. **(7) SYNTHETIC** (SYN) is a synthetically generated graph dataset through the PyTorch Geometric library. This dataset leverages the BA-graph (Barabasi-Albert graph) as its base graph and incorporates HouseMotif and CycleMotif as motif generators, each assigned to separate two classes [62]. One single graph of this dataset contains approximately 0.4 million nodes and 2 million edges.

Classifier. In line with recent works [28, 62, 67, 72], we employ a classic message-passing GNN, namely a graph convolutional network (GCN) with three convolution layers, each having an embedding dimension of 128. To facilitate classification, the GCN model is enhanced with a max pooling layer and a fully connected layer. For datasets without node features, we assign each node a default feature. During training, we utilize the Adam optimizer [34] with a learning rate of 0.001 for 2000 epochs. The datasets are split into 80% for training, 10% for validation, and 10% for testing. The explanations are generated based on the classification results of the test set. Recall that our proposed solutions are model-agnostic, making them adaptable to any GNN employing message-passing.

Competitors. To our best knowledge, GVEX is the first configurable label-level explainer. To demonstrate its effectiveness, we compare it with 4 state-of-the-art GNN explainers, making minor adjustments as necessary to ensure fair comparison. We denote our two-step method as ApproxGVEX (AG) (§4) and our steaming method as SteamGVEX (SG) (§5). **(1) GNNExplainer** (GE) [62] learns soft masks based on mutual information to select critical edges and node features that influence instance-level classification results. **(2) SubgraphX** (SX) [67] employs the Monte Carlo tree search to efficiently explore different subgraphs via node pruning and select the most important subgraph as the explanation for instance-level graph classification. **(3) GStarX** (GX) [72] designs node importance scoring functions using a new structure-aware value from cooperative game theory. It identifies critical nodes and generates an induced subgraph as the explanation for each input graph. **(4) GCFExplainer** (GCF) [28] explores the global explainability of GNNs through counterfactual reasoning. It identifies a set of counterfactual graphs that explain all input graphs of a specific label.

We do not compare against XGNN [65] and PGExplainer [39] since (1) unlike ours and above competitors, XGNN is a model-level explainer, it does not rely on input graphs to generate explanations. As a result, calculating fidelity (see below) becomes difficult. (2) PGExplainer is similar to GNNExplainer, it focuses on edge-level explanation rather than subgraph-level and is not a black box. Therefore, we opted for the more representative method, GNNExplainer.

Evaluation metrics. We evaluate the quality of explanations considering explanation faithfulness and conciseness.

Explanation faithfulness. Fidelity+ and Fidelity- [66] are two widely-used metrics for assessing if explanations are faithful to the model, that is, capable of identifying input features important for the model. Fidelity+ quantifies the deviations caused by a targeted intervention, i.e., removing the

explanation substructure from the input graph.

$$Fidelity+ = \frac{1}{|\mathcal{G}|} \sum_{G \in \mathcal{G}} (Pr(\mathcal{M}(G) = l_G) - Pr(\mathcal{M}(G') = l_G)) \tag{8}$$

where l_G is the original prediction for the graph G. G' represents the updated graph obtained by masking the explanation substructure from the original graph G. Fidelity+ metric measures the difference in probabilities between the new predictions and the original ones. A higher Fidelity+ score indicates better distinction.

In contrast, Fidelity- metric measures how close the prediction results of the explanation substructures are to the original inputs.

$$Fidelity- = \frac{1}{|\mathcal{G}|} \sum_{G \in \mathcal{G}} (Pr(\mathcal{M}(G) = l_G) - Pr(\mathcal{M}(G_s) = l_G)) \tag{9}$$

A desirable Fidelity- score should be close to or even smaller than zero, indicating perfect-matched or even stronger predictions.

We evaluate the explainability of the subgraphs in our explanation views. As clarified earlier in Section 2.2, the "lower-tier" subgraphs are responsible for explaining GNNs with consistent (Fidelity-) and counterfactual (Fidelity+) properties. On the other hand, the "higher-tier" patterns are provided to facilitate better query-ability, as assessed through the following metrics.

Conciseness. To assess the conciseness of explanation subgraphs produced by ours and various competitors, we employ the well-known sparsity metric [66], computed as:

$$Sparsity = \frac{1}{|\mathcal{G}|} \sum_{G \in \mathcal{G}} (1 - \frac{|V_s| + |E_s|}{|V| + |E|}) \tag{10}$$

where the nodes and edges in the input graph G and its explanation subgraph G_s are denoted by (V, E) and (V_s, E_s), respectively. Higher Sparsity values indicate more concise explanations.

Finally, we assess the compression due to "higher level" explanation patterns, which act as summaries of the "lower level" subgraphs. This metric is applicable only for our two-tier explanation views, where the nodes and edges of explanation subgraphs and patterns are denoted as $(\mathbf{V}_S, \mathbf{E}_S)$ and $(\mathbf{V}_\mathcal{P}, \mathbf{E}_\mathcal{P})$, respectively.

$$Compression = 1 - \frac{|\mathbf{V}_\mathcal{P}| + |\mathbf{E}_\mathcal{P}|}{|\mathbf{V}_S| + |\mathbf{E}_S|} \tag{11}$$

6.2 Experimental Results

Exp-1: Effectiveness. Below we report the effectiveness of GVEX.

Explanation faithfulness. To validate the consistency and counterfactual nature of our explanation subgraphs, we generate explanations for one label of user's interest, and vary the configuration constraint u_l to control the maximum number of nodes in explanation subgraphs. For competitors, as they do not have configurable options, we consider their overall qualities for this specific label. If a competitor is absent in the evaluation of a dataset, it indicates that the method took a longer time, i.e., > 24 hours, on that dataset.

Figure 5 and Figure 6 showcase the fidelity metrics with varying u_l. Notably, our proposed ApproxGVEX and StreamGVEX methods consistently outperform all other competitors. They achieve higher Fidelity+ scores (consistent) on all datasets (except for the MUT dataset) and lower Fidelity- scores (counterfactual) on all datasets. Unlike GNNExplainer and SubgraphX, our objective in capturing explainability (Eq. 2) focuses on feature influence and diversity, rather than explicitly optimizing for differences with respect to original prediction results. This shows that our extracted message-passing substructures indeed carry critical information that faithfully corresponds to the classification results.
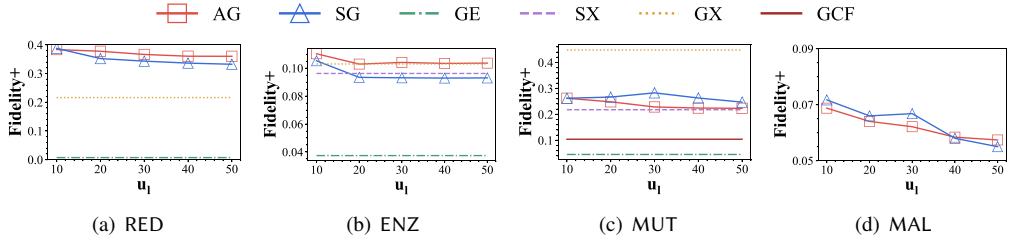
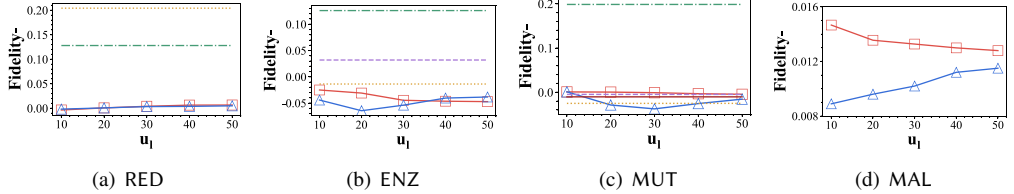Fig. 5. The Fidelity+ comparison across various GNN explainers under different configuration constraints

Fig. 6. The Fidelity- comparison across various GNN explainers under different configuration constraints
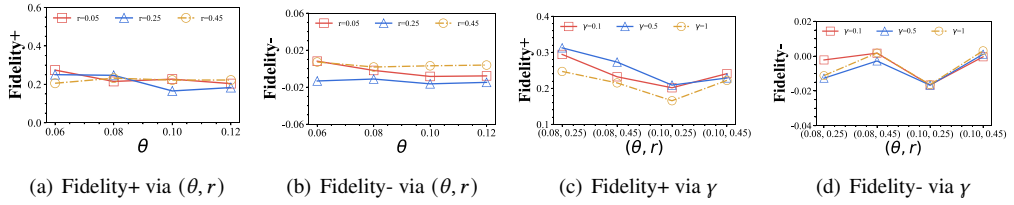

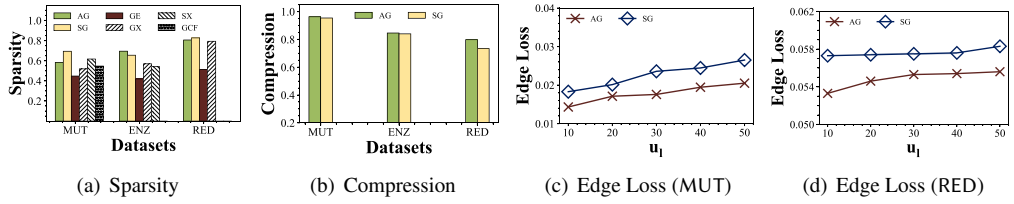Fig. 7. Configuration parameters anayses

Fig. 8. Conciseness analyses

ApproxGVEX and StreamGVEX have minor quality gaps up to 0.023 (Fidelity). StreamGVEX is more fluctuating than ApproxGVEX. For instance, in MAL, the effectiveness of StreamGVEX diminishes more rapidly, falling behind ApproxGVEX when the explanation sizes becomes larger. In contrast, ApproxGVEX maintains a more consistent and uniform trend and performs better due to tighter approximation.

The parameter u_l enforces an upper bound on the size of explanations. Thus, a larger u_l leads to more comprehensive explanations for a class at the expense of higher time cost.

Furthermore, on MUT dataset, we vary the parameters to observe how the fidelity values respond to various combinations of (θ, r). We also adjust the values of γ for the fixed (θ, r) combinations. θ is used to control the boundary of feature influence, r controls the neighborhood diversity, γ is a trade-off between the two. The parameter setting is optimized by grid search. For MUT dataset, we set (θ, r) to $(0.08, 0.25)$ and γ to 0.5. This serves the dual purpose of enabling the algorithm to identify influential nodes possessing diversity while striking a suitable balance between them.

Conciseness. Figure 8(a) depicts the results of sparsity. It is evident that both ApproxGVEX and StreamGVEX consistently generate more compact explanation subgraphs across all datasets. The performance gap can be as high as 0.2 compared to GNNExplainer, which fails to effectively prune

(a) Runtime (MUT)   (b) Runtime (ENZ)   (c) Runtime

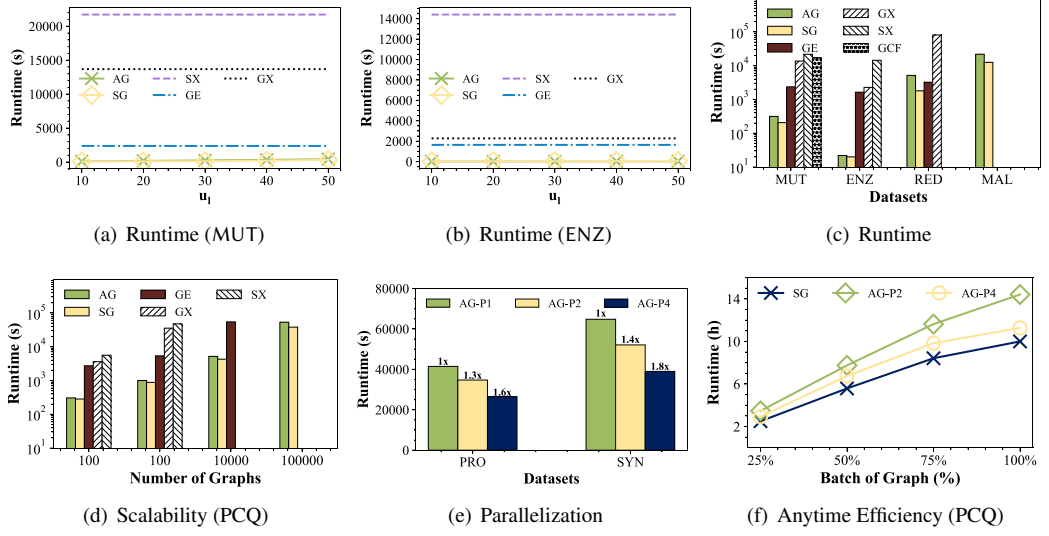(d) Scalability (PCQ)   (e) Parallelization   (f) Anytime Efficiency (PCQ)

Fig. 9. Efficiency, scalability, and parallelization analyses

unessential topological structures. Overall, ApproxGVEX and StreamGVEX significantly reduce the total number of nodes and edges by 60% to 80%, and retain important information to be explored by human experts. ApproxGVEX and StreamGVEX differ only slightly on all datasets because our configuration parameters bound the number of nodes in explanations, which in turn produces slight differences in the number of edges in explanations generated by the two algorithms.

Figure 8(b) demonstrates an excellent reduction in the number of nodes and edges achieved by our "higher-tier" patterns relative to "lower-tier" subgraphs. It reveals that more than 95% of nodes can be further compressed. Recall that our algorithms ensure full coverage of the nodes in the explanation subgraphs by patterns set via node-induced subgraph isomorphism. This observation highlights that the explanation subgraphs can be effectively represented by several significantly smaller substructures. Furthermore, our case study shows that the patterns exhibit significant variation when the labels of interest change. These indicate that GVEX can identify both compact and highly informative patterns, enabling domain experts to explore the critical information from the graphs.

Figure 8(c), 8(d) show the the impact of u_l on edge loss. Edge loss is the percentage of edges that our high-tier patterns fail to cover in the low-tier explanation subgraphs while we satisfy the node coverage constraints in C (see Lemma 4.3). We vary the configuration constraint u_l to control the maximum number of nodes in explanation subgraphs. It depicts that the percentage of edges that the algorithm failed to cover increases when u_l increases. Specifically, in MUT dataset, as u_l varies, the percentage of edges remaining uncovered manifests as $\{1.43\%, 1.71\%, 1.75\%, 1.95\%, 2.10\%\}$.

Exp-2: Efficiency and Scalability. We next demonstrate that our methods consistently generate graph explanations in a more efficient manner, even when dealing with graph databases that have relatively larger individual graphs (e.g., PRO, SYN, MAL) or a large number of graph instances (e.g., PCQ). Figures 9(a)-9(b) present the running times of our ApproxGVEX and StreamGVEX methods, showcasing their significantly faster performance compared to various competitors by 1-2 orders of magnitude. Both ApproxGVEX and StreamGVEX complete their execution within hundreds of seconds on MUT and ENZ, providing substantial improvements in efficiency.

Figure 9(c) provides a more comprehensive overview of the running times of all explainers across various datasets. Notice that all competitors are absent in MAL dataset, which contains relatively larger individual graphs. Additionally, when considering more input graphs on the PCQ dataset,
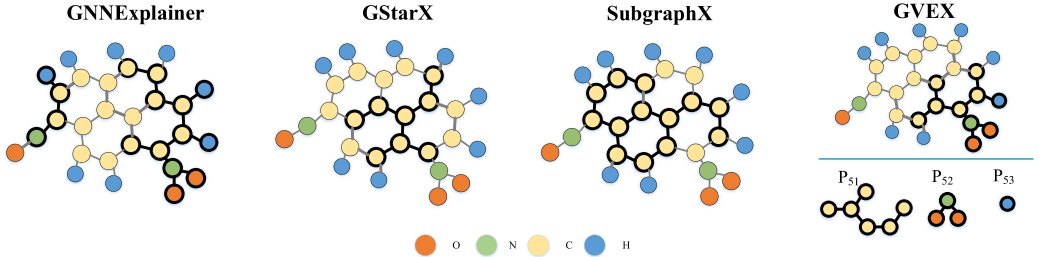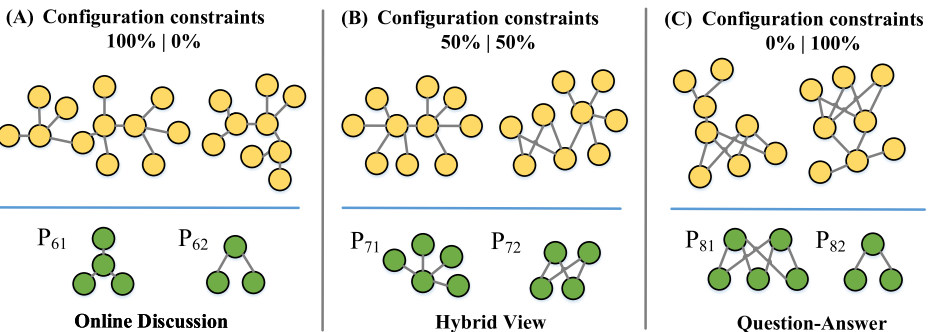
Fig. 10. Case study 1 on GNN-based drug design

Fig. 11. Case study 2 on GNN-based social analysis

all competitors require > 24 hours with 100k graphs as shown in Figure 9(d). In contrast, GVEX successfully completes the task in approximately 8 hours with 100k graphs. These demonstrate the superiority of GVEX solution's in scalability in terms of relatively larger as well as more graphs.

Figure 9(e) shows that our running time reduces by nearly 2× with parallel processing. For PRO dataset, we observe that a node's classification is influenced by message-passing among its neighboring nodes. So we adopt a strategy where we select a specific number of nodes and consider their neighboring nodes to construct subgraphs. The label assigned to a node becomes the label for the entire subgraph. We sample approximately 400 subgraphs, each containing roughly 3000 nodes, resulting in a subgraph classification task involving approximately 1 million nodes and 6 million edges. It takes GVEX about 7 hours to complete this task. For SYN dataset, we use sparse matrix multiplication and random walk technique [3, 12] to optimize the computation on large graphs, and parallelize on multi-processes. With 4 processes, GVEX successfully completes the task in approximately 10 hours. These results demonstrate the efficiency and scalability of the GVEX algorithm when confronted with large, connected graph datasets.

Finally, our streaming method, StreamGVEX, exhibits linear growth in running time with batch size, measued by the percentage of test graphs, making it highly scalable (Figure 9(f)). It also remains more efficient than the 4-processor parallel version of ApproxGVEX, emphasizing its suitability for handling large-scale graph datasets.

Exp-3: Case Studies. In our first case study, we compare the explanation subgraphs identified for one mutagen by different explainers, highlighting them with thicker lines on the input graph (Figure 10). It is evident that GVEX produces smaller subgraphs compared to GNNExplainer and SubgraphX. Furthermore, our explanation view breaks down such subgraphs into smaller components that may appear multiple times, facilitating easier access and exploration. GVEX successfully identifies the real toxicophore, NO_2, allowing for correct and efficient query answering in downstream analytical tasks

such as *"which toxicophore occurs in mutagens?"*. Among the competitors, only GNNExplainer includes NO_2 in its output, albeit with an explanation subgraph consisting of 14 atoms.

Figure 11 provides another case study using the REDDIT-BINARY social network dataset in three different configuration scenarios, where our GVEX explanation view successfully determines representative patterns for different labels of interest. The three configuration scenarios indicate whether the user prefers only one class or is interested in the nature of both classes. For *online-discussion* threads, user interactions typically resemble star-like structures, where many strangers post their thoughts on a popular topic. Our explanation pattern P_{61} aids in distinguishing these topic groups within explanation subgraphs. On the other hand, in *question-answer* threads, users exhibit biclique-like patterns P_{81}, capturing the phenomenon where a few domain experts actively provide answers to various questions raised by different users in closely related domains. When user attempts to understand both classes, GVEX presents the salient patterns of both classes, shedding light on important patterns that underpin the classification of this social network dataset.

7 CONCLUSION

We proposed GVEX, a novel graph view-based two-tier structure to explain GNN-based graph classification. We established hardness results for explanation view generation, and provided efficient algorithms with provable performance guarantees. We experimentally verified that GVEX-based explaination outperforms existing techniques in terms of conciseness, explanability, and efficiency. Our algorithms show good performance on different domains: (social networks, chemistry, biology) and types: (directed/undirected, sparser/denser, with/without node features) of graphs, considering both binary and multi-class classification problems, under static and streaming settings. In future, we shall consider the impact of edge features and develop distributed view-based GNN explanation.

ACKNOWLEDGMENTS

REFERENCES

[1] 2024. Code and datasets. Tingyang Chen, Dazhuo Qiu, Yinghui Wu, Arijit Khan, Xiangyu Ke, and Yunjun Gao. *https://github.com/ZJU-DAILY/GVEX*.

[2] Zahi Ajami and Sara Cohen. 2019. Enumerating minimal weight set covers. In *IEEE International Conference on Data Engineering (ICDE)*. 518–529.

[3] Konstantin Avrachenkov, Nelly Litvak, Danil Nemirovsky, and Natalia Osipova. 2007. Monte Carlo methods in PageRank computation: When one iteration is sufficient. *SIAM J. Numer. Anal.* 45, 2 (2007), 890–904.

[4] Mohit Bajaj, Lingyang Chu, Zi Yu Xue, Jian Pei, Lanjun Wang, Peter Cho-Ho Lam, and Yong Zhang. 2021. Robust counterfactual explanations on graph neural networks. *Advances in Neural Information Processing Systems (NeurIPS)* 34 (2021), 5644–5655.

[5] Karsten M Borgwardt, Cheng Soon Ong, Stefan Schönauer, SVN Vishwanathan, Alex J Smola, and Hans-Peter Kriegel. 2005. Protein function prediction via graph kernels. *Bioinformatics* 21, suppl_1 (2005), i47–i56.

[6] Carrie J Cai, Jonas Jongejan, and Jess Holbrook. 2019. The effects of example-based explanations in a machine learning interface. In *Proceedings of the 24th International Conference on Intelligent User Interfaces*. 258–262.

[7] Gruia Calinescu, Chandra Chekuri, Martin Pal, and Jan Vondrák. 2011. Maximizing a monotone submodular function subject to a matroid constraint. *SIAM J. Comput.* 40, 6 (2011), 1740–1766.

[8] Robert D. Carr, Srinivas Doddi, Goran Konjevod, and Madhav Marathe. 2000. On the red-blue set cover problem. In *ACM-SIAM Symposium on Discrete Algorithms (SODA)*. 345–353.

[9] Amit Chakrabarti and Sagar Kale. 2015. Submodular maximization meets streaming: matchings, matroids, and more. *Mathematical Programming* 154 (2015), 225–247.

[10] Chen Chen, Ye Yuan, Zhenyu Went, Guoren Wang, and Anteng Li. 2022. GQP: A framework for scalable and effective graph query-based pricing. In *IEEE International Conference on Data Engineering (ICDE)*. 1573–1585.

[11] Eunjoon Cho, Seth A Myers, and Jure Leskovec. 2011. Friendship and mobility: user movement in location-based social networks. In *ACM International Conference on Knowledge Discovery and Data Mining (KDD)*. 1082–1090.

[12] Edith Cohen and David D Lewis. 1999. Approximating matrix multiplication for pattern recognition tasks. *Journal of Algorithms* 30, 2 (1999), 211–252.

[13] Enyan Dai and Suhang Wang. 2022. Towards prototype-based self-explainable graph neural network. *arXiv preprint: 2210.01974* (2022).

[14] Marwa El Halabi, Slobodan Mitrović, Ashkan Norouzi-Fard, Jakab Tardos, and Jakub M Tarnawski. 2020. Fairness in streaming submodular maximization: Algorithms and hardness. *Advances in Neural Information Processing Systems (NeurIPS)* 33 (2020), 13609–13622.

[15] Wenfei Fan, Xin Wang, and Yinghui Wu. 2013. Incremental graph pattern matching. *ACM Transactions on Database Systems (TODS)* 38, 3 (2013), 1–47.

[16] Wenfei Fan, Xin Wang, and Yinghui Wu. 2014. Answering graph pattern queries using views. In *IEEE International Conference on Data Engineering (ICDE)*. 184–195.

[17] Peter Floderus, Mirosław Kowaluk, Andrzej Lingas, and Eva-Marta Lundell. 2015. Induced subgraph isomorphism: Are some patterns substantially easier than others? *Theoretical Computer Science* 605 (2015), 119–128.

[18] Scott Freitas, Yuxiao Dong, Joshua Neil, and Duen Horng Chau. 2021. A large-scale database for graph representation learning. In *Proceedings of the Neural Information Processing Systems Track on Datasets and Benchmarks 1, NeurIPS Datasets and Benchmarks*.

[19] Xinyi Gao, Wentao Zhang, Yingxia Shao, Quoc Viet Hung Nguyen, Bin Cui, and Hongzhi Yin. 2022. Efficient graph neural network inference at large scale. *arXiv preprint: 2211.00495* (2022).

[20] Matt Gardner, Joel Grus, Mark Neumann, Oyvind Tafjord, Pradeep Dasigi, Nelson Liu, Matthew Peters, Michael Schmitz, and Luke Zettlemoyer. 2018. Allennlp: A deep semantic natural language processing platform. *arXiv preprint: 1803.07640* (2018).

[21] Stephan Günnemann. 2022. Graph neural networks: Adversarial robustness. *Graph Neural Networks: Foundations, Frontiers, and Applications* (2022), 149–176.

[22] Will Hamilton, Zhitao Ying, and Jure Leskovec. 2017. Inductive representation learning on large graphs. In *Advances in Neural Information Processing Systems (NeurIPS)*. 1024–1034.

[23] Wook-Shin Han, Jinsoo Lee, and Jeong-Hoon Lee. 2013. Turboiso: Towards ultrafast and robust subgraph isomorphism search in large graph databases. In *ACM International Conference on Management of Data (SIGMOD)*. 337–348.

[24] Weihua Hu, Matthias Fey, Hongyu Ren, Maho Nakata, Yuxiao Dong, and Jure Leskovec. 2021. OGB-LSC: A large-scale challenge for machine learning on graphs. In *Proceedings of the Neural Information Processing Systems Track on Datasets and Benchmarks 1, NeurIPS Datasets and Benchmarks*.

[25] Weihua Hu, Matthias Fey, Marinka Zitnik, Yuxiao Dong, Hongyu Ren, Bowen Liu, Michele Catasta, and Jure Leskovec. 2020. Open graph benchmark: Datasets for machine learning on graphs. *Advances in neural information processing systems* 33 (2020), 22118–22133.

[26] Weihua Hu, Matthias Fey, Marinka Zitnik, Yuxiao Dong, Hongyu Ren, Bowen Liu, Michele Catasta, and Jure Leskovec. 2020. Open graph benchmark: Datasets for machine learning on graphs. In *Advances in Neural Information Processing Systems (NeurIPS)*.

[27] Qiang Huang, Makoto Yamada, Yuan Tian, Dinesh Singh, and Yi Chang. 2022. Graphlime: Local interpretable model explanations for graph neural networks. *IEEE Transactions on Knowledge and Data Engineering* (2022).

[28] Zexi Huang, Mert Kosan, Sourav Medya, Sayan Ranu, and Ambuj Singh. 2023. Global counterfactual explainer for graph neural networks. In *ACM International Conference on Web Search and Data Mining (WSDM)*. 141–149.

[29] Anand Padmanabha Iyer, Zaoxing Liu, Xin Jin, Shivaram Venkataraman, Vladimir Braverman, and Ion Stoica. 2018. ASAP: Fast, approximate graph pattern mining at scale. In *13th USENIX Symposium on Operating Systems Design and Implementation (OSDI 18)*. 745–761.

[30] Mingjian Jiang, Zhen Li, Shugang Zhang, Shuang Wang, Xiaofeng Wang, Qing Yuan, and Zhiqiang Wei. 2020. Drug–target affinity prediction using graph neural network and contact maps. *RSC advances* 10, 35 (2020), 20701–20712.

[31] Tim Kaler, Nickolas Stathas, Anne Ouyang, Alexandros-Stavros Iliopoulos, Tao Schardl, Charles E Leiserson, and Jie Chen. 2022. Accelerating training and inference of graph neural networks with fast sampling and pipelining. *Machine Learning and Systems (MLSys)* 4 (2022), 172–189.

[32] Jeroen Kazius, Ross McGuire, and Roberta Bursi. 2005. Derivation and validation of toxicophores for mutagenicity prediction. *Journal of Medicinal Chemistry* 48, 1 (2005), 312–320.

[33] Kyoungmin Kim, In Seo, Wook-Shin Han, Jeong-Hoon Lee, Sungpack Hong, Hassan Chafi, Hyungyu Shin, and Geonhwa Jeong. 2018. Turboflux: A fast continuous subgraph matching system for streaming graph data. In *ACM International Conference on Management of Data (SIGMOD)*. 411–426.

[34] Diederik P Kingma and Jimmy Ba. 2015. Adam: A method for stochastic optimization. In *International Conference on Learning Representations (ICLR)*.

[35] Thomas N Kipf and Max Welling. 2017. Semi-supervised classification with graph convolutional networks. In *International Conference on Learning Representations (ICLR)*.

[36] Johannes Klicpera, Aleksandar Bojchevski, and Stephan Günnemann. 2019. Predict then propagate: Graph neural networks meet personalized pageRank. In *International Conference on Learning Representations (ICLR)*.

[37] Peng Lin, Qi Song, Yinghui Wu, and Jiaxing Pi. 2019. Discovering patterns for fact checking in knowledge graphs. *Journal of Data and Information Quality (JDIQ)* 11, 3 (2019), 1–27.

[38] Yin Lin, Yifan Guan, Abolfazl Asudeh, and HV Jagadish. 2020. Identifying insufficient data coverage in databases with multiple relations. *Proc. VLDB Endow.* 13, 11 (2020).

[39] Dongsheng Luo, Wei Cheng, Dongkuan Xu, Wenchao Yu, Bo Zong, Haifeng Chen, and Xiang Zhang. 2020. Parameterized explainer for graph neural network. *Advances in Neural Information Processing Systems (NeurIPS)* 33 (2020), 19620–19631.

[40] Hanchao Ma, Sheng Guan, Mengying Wang, Yen-shuo Chang, and Yinghui Wu. 2022. Subgraph query generation with fairness and diversity constraints. In *IEEE International Conference on Data Engineering (ICDE)*. 3106–3118.

[41] Imene Mami and Zohra Bellahsene. 2012. A survey of view selection methods. *ACM SIGMOD Record* 41, 1 (2012), 20–29.

[42] Sayan Ranu and Ambuj K Singh. 2009. Graphsig: A scalable approach to mining significant subgraphs in large graph databases. In *2009 IEEE 25th International Conference on Data Engineering*. IEEE, 844–855.

[43] Marcus Schaefer and Christopher Umans. 2002. Completeness in the polynomial-time hierarchy: A compendium. *SIGACT news* 33, 3 (2002), 32–49.

[44] Michael Sejr Schlichtkrull, Nicola De Cao, and Ivan Titov. 2021. Interpreting graph neural networks for nlp with differentiable edge masking. In *International Conference on Learning Representations (ICLR)*.

[45] Robert Schwarzenberg, Marc Hübner, David Harbecke, Christoph Alt, and Leonhard Hennig. 2019. Layerwise relevance visualization in convolutional text graph classifiers. In *Workshop on Graph-Based Methods for Natural Language Processing (TextGraphs@EMNLP)*. 58–62.

[46] Haichuan Shang, Ying Zhang, Xuemin Lin, and Jeffrey Xu Yu. 2008. Taming verification hardness: an efficient algorithm for testing subgraph isomorphism. *Proc. VLDB Endow.* 1, 1 (2008), 364–375.

[47] Qi Song, Yinghui Wu, Peng Lin, Luna Xin Dong, and Hui Sun. 2018. Mining summaries for knowledge graph search. *IEEE Transactions on Knowledge and Data Engineering* 30, 10 (2018), 1887–1900.

[48] Marisa Thoma, Hong Cheng, Arthur Gretton, Jiawei Han, Hans-Peter Kriegel, Alex Smola, Le Song, Philip S Yu, Xifeng Yan, and Karsten M Borgwardt. 2010. Discriminative frequent subgraph mining with optimality guarantees. *Statistical Analysis and Data Mining: The ASA Data Science Journal* 3, 5 (2010), 302–318.

[49] Petar Veličković, Guillem Cucurull, Arantxa Casanova, Adriana Romero, Pietro Lio, and Yoshua Bengio. 2017. Graph attention networks. *arXiv preprint: 1710.10903* (2017).

[50] Sahil Verma, John Dickerson, and Keegan Hines. 2021. Counterfactual explanations for machine learning: Challenges revisited. *arXiv preprint: 2106.07756* (2021).

[51] Lanning Wei, Huan Zhao, Zhiqiang He, and Quanming Yao. 2023. Neural architecture search for GNN-based graph classification. *ACM Transactions on Information Systems* (2023).

[52] Shiwen Wu, Fei Sun, Wentao Zhang, Xu Xie, and Bin Cui. 2022. Graph neural networks in recommender systems: a survey. *Comput. Surveys* 55, 5 (2022), 1–37.

[53] Zonghan Wu, Shirui Pan, Fengwen Chen, Guodong Long, Chengqi Zhang, and S Yu Philip. 2020. A comprehensive survey on graph neural networks. *IEEE Transactions on Neural Networks and Learning Systems* 32, 1 (2020), 4–24.

[54] Jiacheng Xiong, Zhaoping Xiong, Kaixian Chen, Hualiang Jiang, and Mingyue Zheng. 2021. Graph neural networks for automated de novo drug design. *Drug Discovery Today* 26, 6 (2021), 1382–1393.

[55] Keyulu Xu, Weihua Hu, Jure Leskovec, and Stefanie Jegelka. 2019. How powerful are graph neural networks?. In *International Conference on Learning Representations (ICLR)*.

[56] Keyulu Xu, Chengtao Li, Yonglong Tian, Tomohiro Sonobe, Ken-ichi Kawarabayashi, and Stefanie Jegelka. 2018. Representation learning on graphs with jumping knowledge networks. In *International Conference on Machine Learning (ICML)*. 5449–5458.

[57] Han Xuanyuan, Pietro Barbiero, Dobrik Georgiev, Lucie Charlotte Magister, and Pietro Liò. 2023. Global concept-based interpretability for graph neural networks via neuron analysis. In *Proceedings of the AAAI Conference on Artificial Intelligence*, Vol. 37. 10675–10683.

[58] Xifeng Yan, Hong Cheng, Jiawei Han, and Philip S Yu. 2008. Mining significant graph patterns by leap search. In *Proceedings of the 2008 ACM SIGMOD International Conference on Management of Data*. 433–444.

[59] Xifeng Yan and Jiawei Han. 2002. gspan: Graph-based substructure pattern mining. In *IEEE International Conference on Data Mining (ICDM)*. 721–724.

[60] Pinar Yanardag and SVN Vishwanathan. 2015. Deep graph kernels. In *ACM International Conference on Knowledge Discovery and Data Mining (KDD)*. 1365–1374.

[61] Liang Yao, Chengsheng Mao, and Yuan Luo. 2019. Graph convolutional networks for text classification. In *AAAI Conference on Artificial Intelligence*, Vol. 33. 7370–7377.

[62] Zhitao Ying, Dylan Bourgeois, Jiaxuan You, Marinka Zitnik, and Jure Leskovec. 2019. Gnnexplainer: Generating explanations for graph neural networks. *Advances in Neural Information Processing Systems (NeurIPS)* 32 (2019).

[63] Zhitao Ying, Jiaxuan You, Christopher Morris, Xiang Ren, Will Hamilton, and Jure Leskovec. 2018. Hierarchical graph representation learning with differentiable pooling. *Advances in Neural Information Processing Systems (NeurIPS)* 31 (2018).

[64] Jiaxuan You, Bowen Liu, Zhitao Ying, Vijay Pande, and Jure Leskovec. 2018. Graph convolutional policy network for goal-directed molecular graph generation. *Advances in Neural Information Processing Systems (NeurIPS)* 31 (2018).

[65] Hao Yuan, Jiliang Tang, Xia Hu, and Shuiwang Ji. 2020. Xgnn: Towards model-level explanations of graph neural networks. In *ACM international conference on knowledge discovery and data mining (KDD)*. 430–438.

[66] Hao Yuan, Haiyang Yu, Shurui Gui, and Shuiwang Ji. 2023. Explainability in graph neural networks: A taxonomic survey. *IEEE Transactions on Pattern Analysis and Machine Intelligence* 45, 5 (2023), 5782–5799.

[67] Hao Yuan, Haiyang Yu, Jie Wang, Kang Li, and Shuiwang Ji. 2021. On explainability of graph neural networks via subgraph explorations. In *International Conference on Machine Learning (ICML)*. 12241–12252.

[68] Matthew D Zeiler and Rob Fergus. 2014. Visualizing and understanding convolutional networks. In *Computer Vision (ECCV)*. 818–833.

[69] Chao Zhang, Jiaheng Lu, Qingsong Guo, Xinyong Zhang, Xiaochun Han, and Minqi Zhou. 2021. Automatic view selection in graph databases. In *International Conference on Scientific and Statistical Database Management (SSDBM)*. 197–202.

[70] Muhan Zhang and Yixin Chen. 2018. Link prediction based on graph neural networks. *Advances in Neural Information Processing Systems (NeurIPS)* 31 (2018).

[71] Muhan Zhang, Zhicheng Cui, Marion Neumann, and Yixin Chen. 2018. An end-to-end deep learning architecture for graph classification. In *AAAI Conference on Artificial Intelligence*, Vol. 32.

[72] Shichang Zhang, Yozen Liu, Neil Shah, and Yizhou Sun. 2022. GStarX: Explaining graph neural networks with structure-aware cooperative games. In *Advances in Neural Information Processing Systems (NeurIPS)*.

[73] Tianming Zhang, Yunjun Gao, Linshan Qiu, Lu Chen, Qingyuan Linghu, and Shiliang Pu. 2020. Distributed time-respecting flow graph pattern matching on temporal graphs. *World Wide Web* 23 (2020), 609–630.

[74] Wentao Zhang, Zhi Yang, Yexin Wang, Yu Shen, Yang Li, Liang Wang, and Bin Cui. 2021. Grain: Improving data efficiency of graph neural networks via diversified influence maximization. *Proc. VLDB Endow.* 14, 11 (2021), 2473–2482.

[75] Hongkuan Zhou, Ajitesh Srivastava, Hanqing Zeng, Rajgopal Kannan, and Viktor Prasanna. 2021. Accelerating large scale real-time GNN inference using channel pruning. *Proc. VLDB Endow.* 14, 9 (2021).

[76] Marinka Zitnik, Monica Agrawal, and Jure Leskovec. 2018. Modeling polypharmacy side effects with graph convolutional networks. *Bioinformatics* 34, 13 (2018), i457–i466.

A APPENDIX: PROOFS, ALGORITHMS & EXPERIMENTAL STUDY

A.1 Proof of Lemma 3.1

Given a graph database $\mathcal{G}$, configuration C, and a two-tier structure $(\mathcal{P}, \mathcal{G}_s)$, the view verification problem is NP-complete when the GNN $\mathcal{M}$ is fixed.

Proof: It is not hard to verify that view verification is NP-hard, given that it requires subgraph isomorphism tests alone to verify constraint **C1**, which is known to be NP-hard [17].

We next outline an NP algorithm for the verification problem. It performs a three-step verification below. (1) For **C1**, it guesses a finite number of matching functions in PTIME (for patterns $\mathcal{P}$ and $\mathcal{G}$ with bounded size), and verifies if the patterns induce accordingly $\mathcal{G}_s$ via the matching functions in PTIME. If so, $\mathcal{G}_{\mathcal{V}}$ is a graph view. (2) To check **C2**, for each graph $G \in \mathcal{G}$ and its corresponding subgraphs $G_s \in \mathcal{G}_s$, it applies $\mathcal{M}$ to verify if $\mathcal{M}(G_s) = l$ and $\mathcal{M}(G \setminus G_s) \neq l$. If so, $\mathcal{G}_{\mathcal{V}}$ is an explanation view for $\mathcal{G}$. For a fixed GNN $\mathcal{M}$, it takes PTIME to do the inference. (3) It takes PTIME to verify the coverage given that subgraph isomorphism tests have been performed in steps (1) and (2). These verify the upper bound of the verification problem.

A.2 Proof of Theorem 3.2

For a fixed GNN $\mathcal{M}$, EVG is (1) Σ_P^2-complete, and (2) remains NP-hard even when $\mathcal{G}$ has no edges.

Proof: We first show that EVG is solvable in Σ_P^2. We set an **NP** oracle for view verification, which calls the **NP** algorithm in the proof of Lemma 3.1 to check if a pair $(\mathcal{P}, \mathcal{G}_s)$ satisfies the three constraints to be an explanation view under the configuration C for a single label $l \in Ł$ and a single graph $G \in \mathcal{G}$. We outline a second **NP** algorithm below that consults the above **NP** oracle. The nondeterministic algorithm guesses a set of two-tier view structures $\mathcal{G}_\mathcal{V}^l = \{(\mathcal{P}, \mathcal{G}_s)_i\}$ ($i \in [1, |Ł|]$), and determines if for each label group $\mathcal{G}^l$, it contains an explanation view $(\mathcal{P}^l, \mathcal{G}_s^l)$, by calling the above **NP** oracle, in $O(|Ł||\mathcal{P}||\mathcal{G}|)$ time. If so, it then computes $f(\mathcal{G}_\mathcal{V}^l)$ and checks if $f(\mathcal{G}_\mathcal{V}^l) \geq h$ in PTIME.

(2) To see that EVG is Σ_P^2-hard, we construct a reduction from graph satisfiability, a known Σ_P^2-complete problem [43]. Given two sets $\mathcal{G}^+$ and $\mathcal{G}^-$ of graphs with labels '+' and '-' respectively, graph satisfiability problem determines whether there exists a graph G_o such that each graph $G^+ \in \mathcal{G}^+$ is isomorphic to a subgraph of G_o, and each $G^- \in \mathcal{G}^-$ is not isomorphic to any subgraph of G_o. Our reduction assumes that a fixed GNN $\mathcal{M}$ as a binary classifier is provided, and performs a preprocessing step in PTIME as follows. (i) Given an instance of graph satisfiability, we first apply $\mathcal{M}$ to $\mathcal{G}^+$ and $\mathcal{G}^-$ and "regroup" them into two new groups $\mathcal{G}_\mathcal{M}^+$ and $\mathcal{G}_\mathcal{M}^-$, according to the result of $\mathcal{M}$. (ii) We then augment $\mathcal{G}_\mathcal{M}^+$ (resp. $\mathcal{G}_\mathcal{M}^-$) into a new set $\mathcal{G}_\mathcal{M}^{+'}$ (resp. $\mathcal{G}_\mathcal{M}^{-'}$), where for each graph $G_i^+ \in \mathcal{G}_\mathcal{M}^+$ (resp. $G_j^- \in \mathcal{G}_\mathcal{M}^-$), a single independent node v_i^- (resp. v_j^+) with a class label '-' (resp. '+') verified by $\mathcal{M}$ is added, i.e., $\mathcal{M}(v_i) = $ '-' (resp. $\mathcal{M}(v_j) = $ '+'). Such nodes can be obtained with $\mathcal{M}$ inference over all the single nodes (as independent nodes) in $\mathcal{G}$, hence in PTIME. We set graph database $\mathcal{G} = \mathcal{G}_\mathcal{M}^{+'} \cup \mathcal{G}_\mathcal{M}^{-'}$. (3) We set in C the coverage constraints $[|\mathcal{G}_\mathcal{M}^{+'}|, |\mathcal{G}_\mathcal{M}^{+'}|]$ for label '+' (resp. $[0, 0]$ for '-'). One can verify that there exists a solution for graph satisfiability if and only if there is an explanation view for $\mathcal{G}$ that satisfies C.

(3) To see Theorem 3.2(2), we consider a special case of EVG. Let $\mathcal{G}$ contains two single graphs G_1 and G_2, each has no edge. A pre-trained GNN $\mathcal{M}$ as a binary classifier assigns labels on graph nodes (i.e., Ł contains two labels). For such a case, EVG remains to be **NP**-hard. To see this, we construct a reduction from the red-blue set cover problem [8], which is **NP**-complete. This verifies the hardness of EVG for identifying explanation with coverage requirement alone, as in such case, subgraph isomorphism test is no longer intractable.

A.3 Proof of Lemma 3.3

Given $\mathcal{G}$, Ł, C and a fixed GNN $\mathcal{M}$, $f(\mathcal{G}_\mathcal{V})$ is a monotone submodular function.

Proof: As $f(\mathcal{G}_\mathcal{V})$ is the sum of $f(\mathcal{G}_\mathcal{V}^l)$, where l ranges over Ł, and (1) each $f(\mathcal{G}_\mathcal{V}^l)$ is the sum of a node set function $f'(V_{si})$ for each graph G_i in label group $\mathcal{G}^l$, and (2) each $f'(V_{si})$ is in turn only determined by two component node set functions $I(V_{si})$ and $D(V_{si})$, one only needs to show that both its components $I(V_s)$ and $D(V_s)$ are monotone submodular (see Equation 2).

A function $f'(V_s)$ is submodular if for any subsets $V_{s''} \subseteq V_{s'} \subseteq V_s$ and any node $u \notin V_{s'}$, (i) $f'(V_{s''}) \leq f'(V_{s'})$, and (ii) $f'(V_{s''} \cup \{u\}) - f'(V_{s''}) \geq f'(V_{s'} \cup \{u\}) - f'(V_{s'})$ [7].

(1) We first show that $I(\cdot)$ is monotone submodular. Given the node set V_s, we denote as $\mathsf{Inf}(V_s)$ the node set influenced by V_s w.r.t. thresholds (θ, r) (as specified in configuration C); i.e., $I(V_s) = |\mathsf{Inf}(V_s)|$.
(a) Clearly, for any subset $V_{s''} \subseteq V_{s'}$, $\mathsf{Inf}(V_{s''}) \subseteq \mathsf{Inf}(V_s')$, thus $I(V_{s'}) = |\mathsf{Inf}(V_{s'})| \geq |\mathsf{Inf}(V_{s''})| = I(V_{s'})$.
(b) To see its submodularity, we next show that for any set $V_{s''} \subseteq V_{s'}$ and any node $u \notin V_{s'}$,

$$|\mathsf{Inf}(V_{s''} \cup \{u\})| - |\mathsf{Inf}(V_{s''})| \geq |\mathsf{Inf}(V_{s'} \cup \{u\})| - |\mathsf{Inf}(V_{s'})| \tag{12}$$

It then suffices to show that $|\text{Inf}(V_{s'} \cup \{u\})|$ - $|\text{Inf}(V_{s''} \cup \{u\})| \leq |\text{Inf}(V_{s'})|$-$|\text{Inf}(V_{s''})|$. Note that $u \notin V_{s'}$, and $u \notin V_{s''}$. Thus $|\text{Inf}(V_{s'} \cup \{u\})|$ - $|\text{Inf}(V_{s''} \cup \{u\})| = |\text{Inf}(V_{s'}) \cup \text{Inf}(\{u\})|$ - $|\text{Inf}(V_{s''}) \cup \text{Inf}(\{u\})|$. (i) If $\text{Inf}(\{u\}) \cap \text{Inf}(V_{s'}) = \emptyset$, then we have the above equation trivially equals $|\text{Inf}(V_{s'})| + |\text{Inf}(\{u\})|$ - $(|\text{Inf}(V_{s''})| + |\text{Inf}(\{u\})|) = |\text{Inf}(V_{s'})|$ - $|\text{Inf}(V_{s''})|$. (ii) Otherwise, $\text{Inf}(\{u\}) \cap \text{Inf}(V_{s'}) \neq \emptyset$. Note that $|\text{Inf}(V_{s'})|$- $|\text{Inf}(V_{s''})| = |\text{Inf}(V_{s'}) \setminus \text{Inf}(V_{s''})|$. Then, $|\text{Inf}(V_{s'}) \cup \text{Inf}(\{u\})|$ - $|\text{Inf}(V_{s''}) \cup \text{Inf}(\{u\})| = |(\text{Inf}(V_{s'}) \setminus \text{Inf}(V_{s''})) \setminus \text{Inf}(\{u\})| \leq |\text{Inf}(V_{s'}) \setminus \text{Inf}(V_{s''})|$. Putting these together, the submodularity of $I(\cdot)$ hence follows.

(2) Following a similar analysis, we can show that $D(V_s)$ is also monotone submodular. As both $I(V_s)$ and $D(V_s)$ are monotone submodular, and the sum of monotone submodular functions remain to be monotone submodular, Lemma 3.3 follows.

A.4 Proof of Lemma 4.3

For a given set of explanation subgraphs $\mathcal{G}_s^l$, procedure Psum is an H_{u_l}-approximation of optimal $\mathcal{P}^l$ that ensures node coverage (hence satisfies coverage constraint in C). Here, $H_{u_l} = \sum_{i \in [1, C.u_l]} \frac{1}{i}$ is the u_l-th Harmonic number ($C.u_l \geq 1$).

Proof: We show the optimality guarantee by performing a reduction to the minimum weighted set cover problem (MWSC). The problem of MWSC takes as input a universal set X and a set of weighted subsets $\mathcal{X} = \{X_1, \ldots, X_n\}$. Each subset $X_i \in \mathcal{X}$ has a weight w_i. The problem is to select up to k subsets $\mathcal{X}_k \subseteq \mathcal{X} = \{X_1, \ldots X_k\}$ such that $X = \bigcup_{j \in [1,k]} X_j$, with a minimized total sum of weights. (1) Given a set of explanation subgraphs $\mathcal{G}_s^l$, we set the union of the nodes $V_\S$ as X. we consider the pattern candidates $\mathcal{P}$ generated from procedure PGen. For each pattern $P_i \in \mathcal{P}$, we set the node set P_{V_S} that are covered by P in $V_\S$ as a subset X_i, and associate the number of uncovered edges in $\mathcal{G}_s^l$ as $w(P_i)$. This transforms our problem to an instance of an MWSC problem. (2) Given a solution X_k, we simply set $\mathcal{P}^l$ to the set of patterns that are corresponding to the selected subsets in X_k. This transforms the solution back to the solution to our problem. Then we can readily verify the following. (a) The above constructions are in PTIME (in terms of input sizes). (2) Assume there exists a solution X_k that approximates an optimal solution $X*_k$ for MWSC with ratio α, then the corresponding solution $\mathcal{P}^l$ is an α-approximation for our problem. This is because the weights are consistently defined as the edge cover loss for each pattern independently. Given the above analysis, Lemma 4.3 follows.

A.5 Procedure IncUpdateVS

IncUpdateVS consults a greedy swapping strategy to decide whether to replace a node $v' \in V_S$ with v or reject v and put the node v' into V_u. It performs a case analysis: (a) if it can simply adds v to V_S; (b) otherwise, if $\mathcal{P}^l$ already covers v, or v alone does not contribute new patterns to $\mathcal{P}^l$ ($\Delta \mathcal{P} = \emptyset$, as determined by invoke IncPGen), it skips processing v; (c) otherwise, it chooses the node $v' \in V_S$ whose removal has the smallest "loss" of explainability score (Line 1) and replaces v' with v only when such a replacement ensures a gain that is at least twice as much as the loss (Line 2-5). The detail of case(c) is shown in Procedure 4.

A.6 Procedure IncUpdateP

IncUpdateP performs a similar case analysis, yet on patterns $\mathcal{P}^l$, and conducts a swapping strategy to ensure node coverage and small edge misses. For newly maintained V_S, first, ensure meeting node coverage constraints (Line 4-8) by generating new patterns based on the unseen induced explanation subgraph (Line 9-11); second, based on the normalized weight $w(P)$ (Line 12), swapping patterns that have no contribution to the node coverage and have the biggest edge misses (Line 13-14). The detail is shown in Procedure 5.

Procedure 4 IncUpdateVS (v, V_S, V, G, G_s)

1: $v^- := \text{argmin}_{v' \in V_S}(f(V_S) - f(V_S \setminus v'))$
2: $V_u := V_S \setminus \{v^-\}$
3: $w(v) = f(V_u \cup v) - f(V_u); w(v^-) = f(V_u \cup v^-) - f(V_u)$
4: **if** $w(v) \geq 2w(v^-)$ **then**
5:      $V_S := V_S \setminus \{v^-\} \cup \{v\}$
6: **return** V_S

Procedure 5 IncUpdateP $(v, V_S, \mathcal{P}_c)$

1: set $\mathcal{P}' := \emptyset$; v induced subgraph G_{s_v}; and corresponding node set V_v;
2: **for** $v' \in V_S$ **do**
3:      $U := \emptyset$
4:      **for** $P \in \mathcal{P}_c$ **do**
5:          **if** P and $G_{s_{v'}}$ are isomorphic **then**
6:              $U := U \cup \{V_P\}$
7:              **if** $P \notin \mathcal{P}'$ **then**
8:                  $\mathcal{P}' := \mathcal{P}' \cup \{P\}$
9:      **if** $U \neq V_{v'}$ **then**
10:          $P_{new} := G_{s_{v'}}(V_{v'} \setminus U)$
11:          $\mathcal{P}' := \mathcal{P}' \cup P_{new}$
12: $w(P) = 1 - |P_{E_S}| \setminus |E_S|$
13: $\mathcal{P}^- \in \mathcal{P}_c \setminus \mathcal{P}'$ and has biggest $w(\mathcal{P}^-)$
14: $\mathcal{P}_c := \mathcal{P}_c \setminus \mathcal{P}^- \cup \mathcal{P}'$
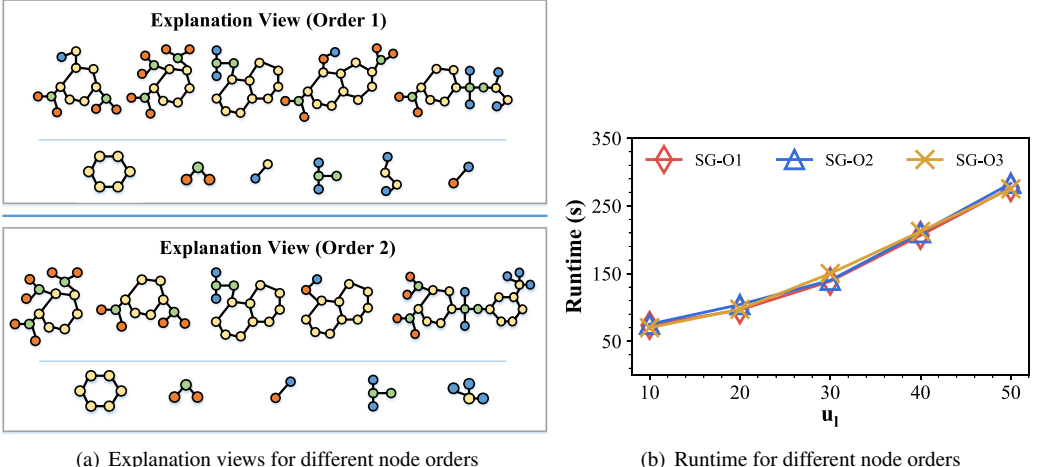15: **return** $\mathcal{P}_c$

A.7 Parallel Implementation

Within our algorithm, the calculation of *Feature Influence* and *Neighborhood Diversity* for each graph is carried out independently. This observation presents a valuable opportunity for the parallelization of our algorithm. Consequently, we are not constrained to relying on a single process to handle all the graphs simultaneously. By employing multi-process execution on a 48-core CPU, we can efficiently distribute the computational load among multiple processes, allowing each process to compute the respective graph autonomously. This approach enables us to enhance the efficiency of the GVEX algorithm. Additionally, these similar concepts can be readily extended to distributed systems.

A.8 Node order analysis w.r.t.StreamGVEX.

The streaming setting does not require a predefined order of nodes. StreamGVEX ascertains an "anytime" quality guarantee, regardless of the node sequences (Theorem 5.1). Our approximation ratio holds w.r.t. an optimal explanation view on the "seen" fraction of $\mathcal{G}$, thus, providing a pragmatic solution for large $\mathcal{G}$. The node arrival sequence inherently impacts the order of pattern discovery, potentially resulting in the early identification of certain patterns. Furthermore, due to our replacement strategies such as IncUpdateVS and IncUpdateP, the arrangement of higher-tier patterns may undergo slight modifications. These strategies intelligently oversee the management of patterns within $\mathcal{P}^l$ through efficient "swapping", allowing for real-time decisions on patterns and node replacement. Consequently, subtle variations may arise in higher-tier patterns contingent upon distinct node processing orders. However, given the approximation guarantee within our algorithm, coupled with the continuous update of pattern information, the vast majority of crucial patterns will persist, even

(a) Explanation views for different node orders

(b) Runtime for different node orders

Fig. 12. Different node orders in StreamGVEX, MUT dataset

under varying node orders, thus exhibiting minimal alterations in the ultimate result. Our additional example (Figure 12(a)) illustrates that there exists a slight difference in the higher-tier patterns from those shown in Figure 4 under different processing orders. Notably, node orders do not affect the worst-case time cost of StreamGVEX. Figure 12(b) validates similar running times on the MUT dataset for various node execution orders obtained via random shuffles.
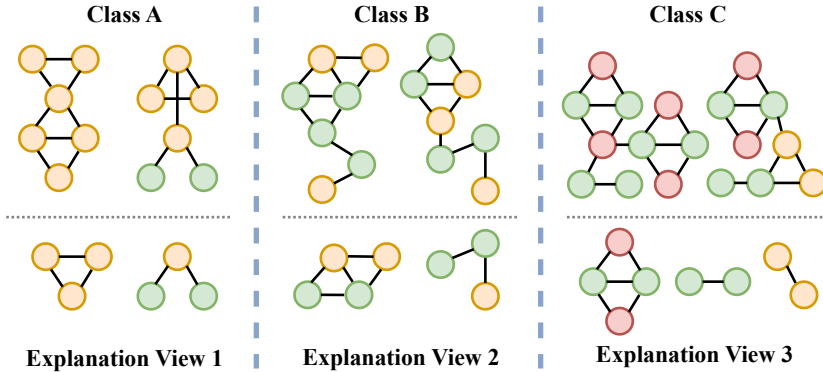

Fig. 13. Explananion views on ENZ dataset

A.9 Case study on ENZYMES.

We further extend the current case studies. We added an analysis of the ENZ dataset (biology), from which three classes are taken out as examples for the generation of the explanation views (Figure 13). This shows that the proposed methods are effective in terms of identifying different subgraph structures.